Inc., Cheltenham, UK). Statistical significance was declared if the *P*-value was <0.05.

Acknowledgements

We are deeply indebted to Professor Kenichi Koike (Department of Pediatrics, Shinshu University School of Medicine) for his excellent advice. We thank Kumiko Sakurai, Yozo Nakazawa, and Jun Miki for their technical assistance, and Daniel Mrozek, Medical English Service Inc, for editorial assistance. This work was supported by grants from the Japanese Ministry of Education, Science, Sports and Culture, Grant-in-Aid for Scientific Research (C) (contract nos: 15591098 and 17591077).

References

Aleyasin H, Cregan SP, Iyirhiaro G, O'Hare MJ, Callaghan SM, Slack RS *et al.* (2004). Nuclear factor-(kappa)B modulates the p53 response in neurons exposed to DNA damage. *J Neurosci* **24**: 2963–2973.

Bell E, Premkumar R, Carr J, Lu X, Lovat PE, Kees UR *et al.* (2006). The role of MYCN in the failure of MYCN amplified neuroblastoma cell lines to G1 arrest after DNA damage. *Cell Cycle* **5**: 2639–2647.

Danial NN, Korsmeyer SJ. (2004). Cell death: critical control points. *Cell* **116**: 205–219.

Green DR. (2000). Apoptotic pathways: paper wraps stone blunts scissors. *Cell* **102**: 1–4.

Hempel G, Flege S, Wurthwein G, Boos J. (2002). Peak plasma concentrations of doxorubicin in children with acute lymphoblastic leukemia or non-Hodgkin lymphoma. *Cancer Chemother Pharmacol* **49**: 133–141.

Hijikata M, Kato N, Sato T, Kagami Y, Shimotohno K. (1990). Molecular cloning and characterization of a cDNA for a novel phorbol-12-myristate-13-acetate-responsive gene that is highly expressed in an adult T-cell leukemia cell line. *J Virol* **64**: 4632–4639.

Hopkins-Donaldson S, Yan P, Bourloud KB, Muhlethaler A, Bodmer JL, Gross N. (2002). Doxorubicin-induced death in neuroblastoma does not involve death receptors in S-type cells and is caspase-independent in N-type cells. *Oncogene* **21**: 6132–6137.

Hudson CD, Morris PJ, Latchman DS, Budhram-Mahadeo VS. (2005). Brn-3a transcription factor blocks p53-mediated activation of proapoptotic target genes Noxa and Bax *in vitro* and *in vivo* to determine cell fate. *J Biol Chem* **280**: 11851–11948.

Isaacs JS, Saito S, Neckers LM. (2001). Requirement for HDM2 activity in the rapid degradation of p53 in neuroblastoma. *J Biol Chem* **276**: 18497–18506.

Kamijo T, Aoyama T, Miyazaki J, Hashimoto T. (1993). Molecular cloning of the cDNAs for the subunits of rat mitochondrial fatty acid beta-oxidation multienzyme complex. Structural and functional relationships to other mitochondrial and peroxisomal beta-oxidation enzymes. *J Biol Chem* **268**: 26452–26460.

Keshelava N, Zuo JJ, Chen P, Waidyaratne SN, Luna MC, Gomer CJ *et al.* (2001). Loss of p53 function confers high-level multidrug resistance in neuroblastoma cell lines. *Cancer Res* **61**: 6185–6193.

Kiryu-Seo S, Hirayama T, Kato R, Kiyama H. (2005). Noxa is a critical mediator of p53-dependent motor neuron death after nerve injury in adult mouse. *J Neurosci* **25**: 1442–1447.

Komarova EA, Chernov MV, Franks R, Wang K, Armin G, Zelnick CR *et al.* (1997). Transgenic mice with p53-responsive lacZ: p53 activity varies dramatically during normal development and determines radiation and drug sensitivity *in vivo*. *EMBO J* **16**: 1391–1400.

Letai A, Bassik MC, Walensky LD, Sorcinelli MD, Weiler S, Korsmeyer SJ. (2002). Distinct BH3 domains either sensitize or activate mitochondrial apoptosis, serving as prototype cancer therapeutics. *Cancer Cell* **2**: 183–192.

Lee SJ, Kim KM, Namkoong S, Kim CK, Kang YC, Lee H *et al.* (2005). Nitric oxide inhibition of homocysteine-induced human endothelial cell apoptosis by down-regulation of p53-dependent Noxa expression through the formation of S-nitrosohomocysteine. *J Biol Chem* **280**: 5781–5788.

Lowe SW, Bodis S, McClatchey A, Remington L, Ruley HE, Fisher DE *et al.* (1994). p53 status and the efficacy of cancer therapy *in vivo*. *Science* **266**: 807–810.

Machida T, Fujita T, Ooo ML, Ohira M, Isogai E, Mihara M *et al.* (2006). Increased expression of proapoptotic BMCC1, a novel gene with the BNIP2 and Cdc42GAP homology (BCH) domain, is associated with favorable prognosis in human neuroblastomas. *Oncogene* **25**: 1931–1942.

Matthay KK, Perez C, Seeger RC, Brodeur GM, Shimada H, Atkinson JB *et al.* (1998). Successful treatment of stage III neuroblastoma based on prospective biologic staging: a Children's Cancer Group study. *J Clin Oncol* **16**: 1256–1264.

Moll UM, LaQuaglia M, Bénard J, Riou G. (1995). Wild-type p53 protein undergoes cytoplasmic sequestration in undifferentiated neuroblastomas but not in differentiated tumors. *Proc Natl Acad Sci USA* **92**: 4407–4411.

Moll UM, Ostermeyer AG, Haladay R, Winkfield B, Frazier M, Zambetti G. (1996). Cytoplasmic sequestration of wild-type p53 protein impairs the G1 checkpoint after DNA damage. *Mol Cell Biol* **16**: 1126–1137.

Nakazawa Y, Kamijo T, Koike K, Noda T. (2003). ARF tumor suppressor induces mitochondria-dependent apoptosis by modulation of mitochondrial Bcl-2 family proteins. *J Biol Chem* **278**: 27888–27895.

Obexer P, Geiger K, Ambros PF, Meister B, Ausserlechner MJ. (2007). FKHRL1-mediated expression of Noxa and Bim induces apoptosis via the mitochondria in neuroblastoma cells. *Cell Death Diff* **14**: 534–547.

Oda E, Ohki R, Murasawa H, Nemoto J, Shibue T, Yamashita T *et al.* (2003). Noxa, a BH3-only member of the Bcl-2 family and candidate mediator of p53-induced apoptosis. *Science* **17**: 1053–1058.

Oda K, Arakawa H, Tanaka T, Matsuda K, Tanikawa C, Mori T *et al.* (2000). p53AIP1, a potential mediator of p53-dependent apoptosis, and its regulation by Ser-46-phosphorylated p53. *Cell* **102**: 849–862.

Ohtani S, Kagawa S, Tango Y, Umeoka T, Tokunaga N, Tsunemitsu Y *et al.* (2004). Quantitative analysis of p53-targeted gene expression and visualization of p53 transcriptional activity following intratumoral administration of adenoviral p53 *in vivo*. *Mol Cancer Ther* **3**: 93–100.

Oren M. (1999). Regulation of the p53 tumor suppressor protein. *J Biol Chem* **274**: 36031–36034.

Paull AC, Whikehart DR. (2005). Regulation of the p53 tumor suppressor protein. *Mol Vis* **11**: 328–334.

Qin JZ, Stennett L, Bacon P, Bodner B, Hendrix MJ, Seftor RE *et al.* (2004). p53-independent NOXA induction overcomes apoptotic resistance of malignant melanomas. *Mol Cancer Ther* **3**: 895–902.

Shen Y, White E. (2001). p53-dependent apoptosis pathways. *Adv Cancer Res* **82**: 55–84.

Shibue T, Takeda K, Oda E, Tanaka H, Murasawa H, Takaoka A *et al.* (2003). Integral role of Noxa in p53-mediated apoptotic response. *Genes Dev* **17**: 2233–2238.

Shieh SY, Ikeda M, Taya Y, Prives C. (1997). DNA damage-induced phosphorylation of p53 alleviates inhibition by MDM2. *Cell* **91**: 325–334.

Tweddle DA, Malcolm AJ, Bown N, Pearson AD, Lunec J. (2001). Evidence for the development of p53 mutations after cytotoxic therapy in a neuroblastoma cell line. *Cancer Res* **61**: 8–13.

Tweddle DA, Pearson AD, Haber M, Norris MD, Xue C, Flemming C *et al.* (2003). The p53 pathway and its inactivation in neuroblastoma. *Cancer Lett* **197**: 93–98.

Wong HK, Fricker M, Wyttenbach A, Villunger A, Michalak EM, Strasser A *et al.* (2005). Mutually exclusive subsets of BH3-only proteins are activated by the p53 and c-Jun N-terminal kinase/c-Jun signaling pathways during cortical neuron apoptosis induced by arsenite. *Mol Cell Biol* **25**: 8732–8747.

Wei MC, Zong WX, Cheng EH, Lindsten T, Panoutsakopoulou V, Ross AJ *et al.* (2001). Proapoptotic BAX and BAK: a requisite gateway to mitochondrial dysfunction and death. *Science* **292**: 727–730.

Wolff A, Technau A, Ihling C, Technau-Ihling K, Erber R, Bosch FX *et al.* (2001). Evidence that wild-type p53 in neuroblastoma cells is in a conformation refractory to integration into the transcriptional complex. *Oncogene* **20**: 1307–1317.

Yakovlev AG, Di Giovanni S, Wang G, Liu W, Stoica B, Faden AI. (2004). BOK and NOXA are essential mediators of p53-dependent apoptosis. *J Biol Chem* **279**: 28367–28374.

THE JOURNAL OF BIOLOGICAL CHEMISTRY VOL. 283, NO. 7, pp. 3979–3987, February 15, 2008

Activation of AMP-activated Protein Kinase Induces p53-dependent Apoptotic Cell Death in Response to Energetic Stress*[S]

Received for publication, June 26, 2007, and in revised form, September 12, 2007 Published, JBC Papers in Press, December 4, 2007, DOI 10.1074/jbc.M705232200

Rintaro Okoshi[‡§], Toshinori Ozaki[‡], Hideki Yamamoto[‡], Kiyohiro Ando[‡], Nami Koida[‡], Sayaka Ono[¶], Tadayuki Koda[¶], Takehiko Kamijo[‡], Akira Nakagawara[‡1], and Harutoshi Kizaki[§2]

From the [‡]Division of Biochemistry, Chiba Cancer Center Research Institute, Chiba 260-8717, [§]Oral Health Science Center, Tokyo Dental College, Chiba 261-8502, and [¶]Center for Functional Genomics, Hisamitsu Pharmaceutical Co., Inc., Chiba 260-8717, Japan

Tumor suppressor p53-dependent stress response pathways play an important role in cell fate determination. In this study, we have found that glucose depletion promotes the phosphorylation of AMP-activated protein kinase catalytic subunit α (AMPKα) in association with a significant up-regulation of p53, thereby inducing p53-dependent apoptosis *in vivo* and *in vitro*. Thymocytes prepared from glucose-depleted wild-type mice but not from p53-deficient mice underwent apoptosis, which was accompanied by a remarkable phosphorylation of AMPKα and a significant induction of p53 as well as pro-apoptotic Bax. Similar results were also obtained in human osteosarcoma-derived U2OS cells bearing wild-type *p53* following glucose starvation. Of note, glucose deprivation led to a significant accumulation of p53 phosphorylated at Ser-46, but not at Ser-15 and Ser-20, and a transcriptional induction of *p53* as well as pro-apoptotic *p53 AIP1*. Small interference RNA-mediated knockdown of p53 caused an inhibition of apoptosis following glucose depletion. Additionally, apoptosis triggered by glucose deprivation was markedly impaired by small interference RNA-mediated depletion of AMPKα. Under our experimental conditions, down-regulation of AMPKα caused an attenuation of p53 accumulation and its phosphorylation at Ser-46. In support of these observations, enforced expression of AMPKα led to apoptosis and resulted in an induction of p53 at protein and mRNA levels. Furthermore, *p53* promoter region responded to AMPKα and glucose deprivation as judged by luciferase reporter assay. Taken together, our present findings suggest that AMPK-dependent transcriptional induction and phosphorylation of p53 at Ser-46 play a crucial role in the induction of apoptosis under carbon source depletion.

AMP-activated protein kinase (AMPK)[3] was originally identified as an enzyme that has an ability to inhibit hydroxymethylglutaryl-CoA reductase (1) and also regulate acetyl-CoA carboxylase by reversible phosphorylation (2). Subsequent studies demonstrated that AMPK is widely expressed and exists as a heterotrimeric complex, which consists of a catalytic subunit (α) and two regulatory subunits (β and γ). The mammalian genome contains seven *AMPK* genes encoding two α (α1 and α2), two β (β1 and β2), and three γ (γ1, γ2, and γ3) isoforms (3–5). The catalytic α subunit is composed of three functional domains, including an NH_2-terminal Ser/Thr protein kinase domain, a central auto-inhibitory region, and a COOH-terminal regulatory subunit-binding domain. AMPK acts as an intracellular energy sensor by monitoring cellular energy levels. For example, AMPK becomes activated by the tumor suppressor LKB1 complex-mediated phosphorylation at Thr-172 in response to certain energy-depleting stresses such as glucose deprivation, hypoxia, and oxidative stress, which increase the intracellular AMP:ATP ratio (6–10). AMPK can also be activated allosterically in the AMP:ATP ratio (11). Upon activation, AMPK down-regulates the ATP consuming metabolic pathways and activates the energy-generating processes through phosphorylating the primary targets involved in energy metabolism, thereby maintaining energy balance within cells (4).

Pro-apoptotic p53 is a founding member of the p53 tumor suppressor family and acts as a critical regulator of many cellular processes such as cell cycle arrest and apoptosis (12). *p53* is frequently mutated in over 50% of human tumors (13–15), and p53-deficient mice developed spontaneous tumors (16). p53 acts as a nuclear sequence-specific transcription factor and transactivates its numerous target genes implicated in cell cycle arrest and apoptotic cell death, including $p21_{WAF1}$, *Bax*, *Puma*, *Noxa*, and *p53 AIP1*. Its pro-apoptotic function is closely linked to its DNA binding activity. Indeed, over 90% of the p53 mutation is detected within its sequence-specific DNA-binding domain (13–15). Intracellular p53 protein levels are tightly regulated predominantly through the ubiquitin-proteasome protein degradation pathway. MDM2, which interacts with the NH_2-terminal transactivation domain of p53 and inhibits its

* This work was supported in part by a grant-in-aid from the Ministry of Health, Labor and Welfare for Third Term Comprehensive Control Research for Cancer, a grant-in-aid for scientific research on priority areas from the Ministry of Education, Culture, Sports, Science and Technology, Japan, a grant-in-aid for scientific research from Japan Society for the Promotion of Science, and a grant from Uehara Memorial Foundation. The costs of publication of this article were defrayed in part by the payment of page charges. This article must therefore be hereby marked "*advertisement*" in accordance with 18 U.S.C. Section 1734 solely to indicate this fact.

[S] The on-line version of this article (available at http://www.jbc.org) contains supplemental Figs. S1 and S2.

[1] To whom correspondence may be addressed. Tel.: 81-43-264-5431; Fax: 81-43-265-4459; E-mail: akiranak@chiba-cc.jp.

[2] To whom correspondence may be addressed. Tel.: 81-43-270-3750; Fax: 81-43-270-3752; E-mail: kizaki@tdc.ac.jp.

[3] The abbreviations used are: AMPK, AMP-activated protein kinase; DAPI, 4,6-diamidino-2-phenylindole; FACS, fluorescence-activated cell sorter; FBS, fetal bovine serum; *GAPDH*, glyderaldehyde-3-phosphate dehydrogenase; IB, immunoblotting; PARP, poly(ADP-ribose) polymerase; PBS, phosphate-buffered saline; RT, reverse transcription; siRNA, small interference RNA.

transcriptional activity, is one of the ubiquitin-protein isopeptide ligases for p53 (17, 18). In response to various types of cellular stress, including DNA damage, hypoxia, nucleotide pool reduction, and thermal shock, p53 is induced to be stabilized as well as activated in the cell nucleus, and thereby plays a key role in the regulation of cell fate determination (19–21). Recently, it has been shown that cells treated with low glucose arrest in the G_1 phase of the cell cycle in association with a significant activation of AMPK (22). According to their results, AMPK-mediated cell cycle arrest in response to low glucose required the phosphorylation of tumor suppressor p53 at Ser-15. Because stress-induced phosphorylation of p53 at Ser-15, which disrupts the p53-MDM2 interaction, enhances its activity as well as stability (19–21), it is likely that p53 plays an important role in the regulation of cell cycle arrest caused by glucose limitation. Indeed, p53-deficient cells failed to arrest under low glucose conditions (22). Consistent with these results, activation of AMPK in human hepatocellular carcinoma-derived HepG2 cells bearing wild-type *p53* resulted in G_1 cell cycle arrest through stabilization of p53 (23). Previously, Stefanelli *et al.* (24) described that AMPK has a protective role against thymocyte apoptosis in response to dexamethasone treatment.

In this study, we have found that glucose deprivation induces phosphorylation of AMPKα and promotes p53-dependent apoptotic cell death *in vivo* and *in vitro*. Under our experimental conditions, p53 was induced in response to glucose depletion at mRNA and at protein levels. Our present findings suggest that AMPK acts as a metabolic sensor to determine cell fate through the activation of pro-apoptotic p53.

EXPERIMENTAL PROCEDURES

Mice—Six-week-old male c57BL/6 mice (23–24 g), which were purchased from Charles River Laboratories (Tokyo, Japan), were housed in an animal facility maintained on a 12-h light/dark cycle at a constant temperature of 22 ± 1 °C and given free access to food and water *ad libitum*. For starvation, food was withdrawn from the cages at the onset of the dark cycle for the indicated times, whereas access to water was allowed. All experiments with these mice were carried out with the approval of the Chiba Cancer Center Experimental Animal Care and Use Committee.

Cell Lines and Transfection—Human osteosarcoma-derived U2OS cells were maintained in Dulbecco's modified Eagle's medium supplemented with 10% heat-inactivated fetal bovine serum (FBS; Invitrogen), 50 μg/ml penicillin, and 50 μg/ml streptomycin (Invitrogen). Human lung carcinoma H1299 cells were grown in RPMI 1640 medium supplemented with 10% heat-inactivated FBS plus antibiotics mixture. These cells were cultured in a humidified atmosphere of 5% CO_2, 95% air at 37 °C. Where indicated, U2OS cells were cultured in glucose-free Dulbecco's modified Eagle's medium (Invitrogen) supplemented with 10% dialyzed FBS. For transient transfection, U2OS and H1299 cells were transfected with the indicated combinations of the expression plasmids using Lipofectamine 2000 transfection reagent (Invitrogen) according to the manufacturer's instructions. pcDNA3 (Invitrogen) was used as a blank plasmid to balance the amount of DNA introduced in transient transfection.

RNA Extraction and RT-PCR—Total RNA was prepared from the indicated cells by using the RNeasy mini kit (Qiagen, Valencia, CA), according to the manufacturer's protocol, and reverse-transcribed with SuperScript II reverse transcriptase (Invitrogen). The resultant cDNA was amplified by PCR with rTaq DNA polymerase (Takara, Ohtsu, Japan) using the following primers: p53, 5′-CTGCCCTCAACAAGATGTTTTG-3′ (forward) and 5′-CTATCTGAGCAGCGCTCATGG-3′ (reverse); $p21^{WAF1}$, 5′-ATGAAATTCACCCCCTTTCC-3′ (forward) and 5′-CCCTAGGCTGTGCTCACTTC-3′ (reverse); Bax, 5′-TTTGCTTCAGGGTTTCATCC-3′ (forward) and 5′-CAGTTGAAGTTGCCGTCAGA-3′ (reverse); *p53 AIP1*, 5′-TGGCTCCAGGAAGGAAAGGC-3′ (forward) and 5′-TGCTTTCTGCAGACAGGGCC-3′ (reverse); AMPKα1, 5′-CAGGGACTGCTACTCCACAGAGA-3′ (forward) and 5′-CCTTGAGCCTCAGCATCTGAA-3′ (reverse); AMPKα2, 5′-CAACTGCAGAGAGCCATTCACTT-3′ (forward) and 5′-GGTGAAACTGAAGACAATGTGCTT-3′ (reverse); and GAPDH, 5′-ACCTGACCTGCCGTCTAGAA-3′ (forward) and 5′-TCCACCACCCTGTTGCTGTA-3′ (reverse). The expression of *GAPDH* was measured as an internal control.

Immunoblotting—Cells were scraped off the plates and transferred into the microcentrifuge tubes. The cells were then lysed in lysis buffer containing 10 mM Tris-HCl, pH 8.0, 150 mM NaCl, 2 mM EGTA, 50 mM β-mercaptoethanol ,1% Triton X-100, a commercial protease inhibitor mixture (Sigma) and phosphatase inhibitor mixture (Sigma) for 30 min on ice, and subjected to a brief sonication for 10 s at 4 °C followed by centrifugation at 15,000 rpm at 4 °C for 10 min to remove insoluble materials. The protein concentrations were measured using the Bradford protein assay according to the manufacturer's instructions (Bio-Rad). The equal amounts of protein (20 μg) were separated by 10% SDS-PAGE and electrophoretically transferred onto polyvinylidene difluoride membranes (Immobilon-P, Millipore, Bedford, MA). The transferred membranes were blocked with Tris-buffered saline containing 5% nonfat dry milk and 0.1% Tween 20 at 4 °C overnight. After blocking, the membranes were incubated with monoclonal anti-p53 (DO-1; Oncogene Research Products, Cambridge, MA), monoclonal anti-Bax (6A7; eBioscience, San Diego, CA), polyclonal anti-phospho-p53 at Ser-15 (Cell Signaling, Beverly, MA), polyclonal anti-phospho-p53 at Ser-20 (Cell Signaling), polyclonal anti-phospho-p53 at Ser-46 (Cell Signaling), polyclonal anti-$p21^{WAF1}$ (H-164; Santa Cruz Biotechnology), polyclonal anti-AMPKα (Cell Signaling), polyclonal anti-phospho-AMPKα (Cell Signaling), polyclonal anti-PARP (Cell Signaling), or with polyclonal anti-actin (20–33; Sigma) antibody for 1 h at room temperature. After incubation with primary antibodies, the membranes were incubated with horseradish peroxidase-coupled goat anti-mouse or anti-rabbit IgG secondary antibody (Cell Signaling) for 1 h at room temperature. Immunoblots were visualized by ECL detection reagents according to the manufacturer's instructions (Amersham Biosciences).

Immunoprecipitation—At the indicated time points after glucose depletion, whole cell lysates prepared from U2OS cells

were pre-cleared with 30 μl of protein G-Sepharose beads for 90 min at 4 °C, and supernatants were incubated with the indicated antibodies overnight at 4 °C. After incubation, the reaction mixtures were mixed with 30 μl of protein G-Sepharose beads and incubated for 1 h at 4 °C. The immune complexes were eluted with SDS-sample buffer, and separated by 10% SDS-PAGE followed by immunoblotting with the indicated antibodies.

Indirect Immunofluorescence Microscopy—U2OS cells were cultured in the absence of glucose. At the indicated times after glucose deprivation, cells were fixed in 3.7% formaldehyde for 30 min at room temperature, permeabilized in 0.2% Triton X-100 for 5 min at room temperature, and then blocked with 3% bovine serum albumin in phosphate-buffered saline (PBS) for 1 h at room temperature. After blocking, cells were washed in PBS and incubated with polyclonal anti-phospho-AMPKα and monoclonal anti-p53 or with polyclonal anti-phospho-AMPKα and monoclonal anti-nucleolin antibodies (StressGen Biotechnologies, Cambridge, UK) for 1 h at room temperature, followed by the incubation with fluorescein isothiocyanate-conjugated anti-rabbit IgG and rhodamine-conjugated anti-mouse IgG (Invitrogen) for 1 h at room temperature. Cell nuclei were stained with DAPI. The specific fluorescence was observed by using a confocal laser scanning microscope (Olympus, Tokyo, Japan).

Flow Cytometry—After glucose deprivation, both floating and attached cells were collected by low speed centrifugation and washed in PBS. The cells were treated with 500 μg/ml of RNase A (Sigma) and subsequently stained with 50 μg/ml of propidium iodide (Sigma) for 30 min at room temperature. Then the DNA content indicated by propidium iodide staining was analyzed by FACSCalibur flow cytometer (BD Biosciences).

Luciferase Reporter Assay—p53-deficient H1299 cells were plated in 12-well plates at a density of 50,000 cells/well and transiently co-transfected with a constant amount of a luciferase reporter construct driven by the *p53* promoter (100 ng) and 10 ng of *Renilla* luciferase expression plasmid (pRL-TK) together with or without the increasing amounts of the expression plasmids for AMPKα1 plus AMPK α2 (50, 100, or 200 ng). For all transfections, the total DNA amounts were kept constant (510 ng) using empty parental plasmid. Forty eight hours after transfection, cells were lysed, and their luciferase activities were measured by dual luciferase reporter assay system (Promega, Madison, WI). Results represent an average firefly luciferase value after normalization to *Renilla* luciferase signal. Each experiment was performed at least three times by triplicates.

Construction of the Expression Plasmids for AMPKα1 and AMPKα2—To generate the expression plasmids for AMPKα1 and AMPKα2, we employed PCR-based amplification using cDNA prepared from U2OS cells as a template. For AMPKα1, the 5′-part of the entire coding region was amplified by PCR using the following primer sequences: 5′-GGAATTCCATGCGCAGACTCAGTTCCTG-3′ and 5′-CTGCAGCATATGTTTCAAAAG-3′, which include EcoRI and PstI restriction sites, respectively. The 3′-part of the entire coding region was also amplified by PCR using the following primer sequences: 5′-CTGCAGGTGGATCCCATGAAG-3′ and 5′-CCGCTCGAGCGGTTATTGTGCAAGAATTT-3′, which contain PstI and XhoI restriction sites, respectively. The resultant 5′- and 3′-parts of the entire coding regions were digested completely with EcoRI and PstI or with PstI and XhoI, respectively, and subcloned into EcoRI and XhoI restriction sites of pcDNA3 (Invitrogen) to give pcDNA3-AMPKα1. For AMPKα2, the 5′-part of the entire coding region was amplified by PCR using the following primer sequences: 5′-CGGGATCCCGATGGCTGAGAGAAGCAGAAGC-3′ and 5′-ACTAGTTCTCAGAAATTCAC-3′, which include BamHI and SpeI restriction sites, respectively. The 3′-part of the entire coding region was also amplified by PCR using the following primer sequences: 5′-ACTAGTTGCGGATCTCCAAATTATAC-3′ and 5′-GGAATTCCTCAACGGGCTAAAGTAGTAGTAATC-3′, which contain SpeI and EcoRI restriction sites, respectively. The amplified PCR products corresponding to 5′- or 3′-part of the entire coding region were treated with BamHI and SpeI or with SpeI and EcoRI, respectively, and introduced into BamHI and EcoRI sites of pcDNA3 (Invitrogen) to give pcDNA3-AMPKα2. Nucleotide sequences of the PCR products were determined to verify the absence of random mutations.

RNA Interference—To knock down the endogenous AMPKα, U2OS cells were transiently transfected with 10 nM of the chemically synthesized siRNAs targeting AMPKα1 and AMPKα2 or with the nonsilencing control siRNA (Invitrogen) using Lipofectamine™ RNAiMAX (Invitrogen) according to the manufacturer's recommendations. Total RNA and whole cell lysates were prepared 48 h after transfection. siRNA sequences used in the present study are available upon request.

RESULTS

Glucose Depletion Induces Apoptotic Cell Death in Vivo and in Vitro—To examine whether glucose depletion could induce apoptotic cell death *in vivo*, we have prepared thymocytes from wild-type and *p53*-deficient mice that were maintained in the absence of glucose for 24 h, and their cell cycle distributions were analyzed by FACS. As shown in Fig. 1*A*, glucose deprivation resulted in a significant increase in number of thymocytes with sub-G_1 DNA content in wild-type mice, whereas glucose depletion had undetectable effects on thymocytes derived from *p53*-deficient mice, indicating that glucose deprivation-mediated apoptotic cell death might be regulated in a p53-dependent manner. Consistent with the previous observations (22), glucose depletion promoted the extensive phosphorylation of AMPKα in wild-type thymocytes (Fig. 1*B*). Under our experimental conditions, p53 accumulated in response to glucose starvation. Intriguingly, the accumulation of p53 was clearly associated with a significant induction of AMPKα phosphorylation as well as pro-apoptotic Bax, which is one of the direct targets of p53 (19–21). Additionally, proteolytic cleavage of PARP, which is one of the substrates of the activated caspase-3, was induced in response to glucose deprivation. In contrast, the expression levels of $p21^{WAF1}$, which have been shown to be implicated in p53-dependent cell cycle arrest (19–21), remained almost unchanged regardless of glucose deprivation.

To further confirm this issue *in vitro*, human osteosarcoma-derived U2OS cells bearing wild-type *p53* were cultured in medium completely deficient in glucose for the indicated times,

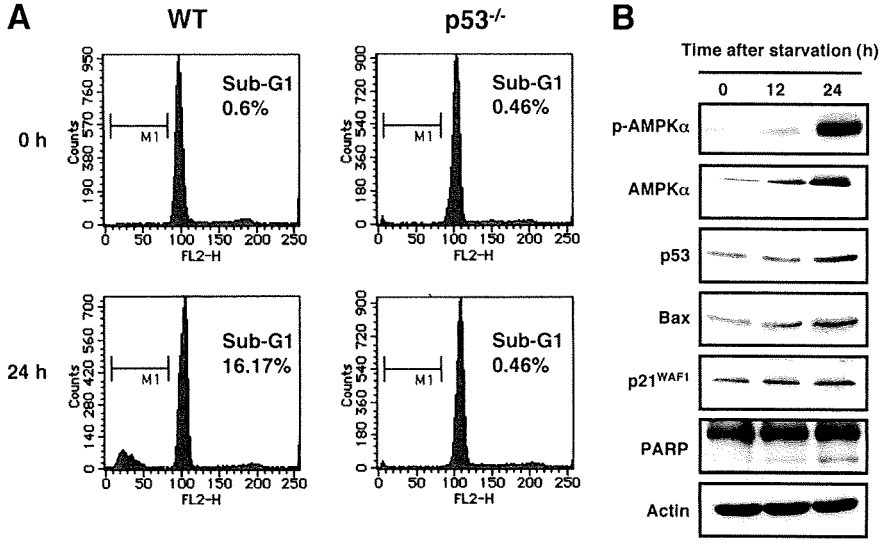

FIGURE 1. **Glucose depletion induces apoptotic cell death in mouse thymocytes.** *A*, FACS analysis. Thymocytes prepared from wild-type (*WT*) mice (*left*) or from p53-deficient mice (*right*) maintained under glucose deprivation conditions for 24 h were stained with propidium iodide and subjected to FACS analysis to determine the number of thymocytes with sub-G_1 DNA content. *B*, AMPKα is induced to be phosphorylated in response to glucose deprivation. Thymocytes were prepared from wild-type mice at the indicated times after glucose removal and subjected to immunoblotting (IB) with the indicated antibodies. Blot was also probed with anti-actin antibody to confirm equal loading of samples.

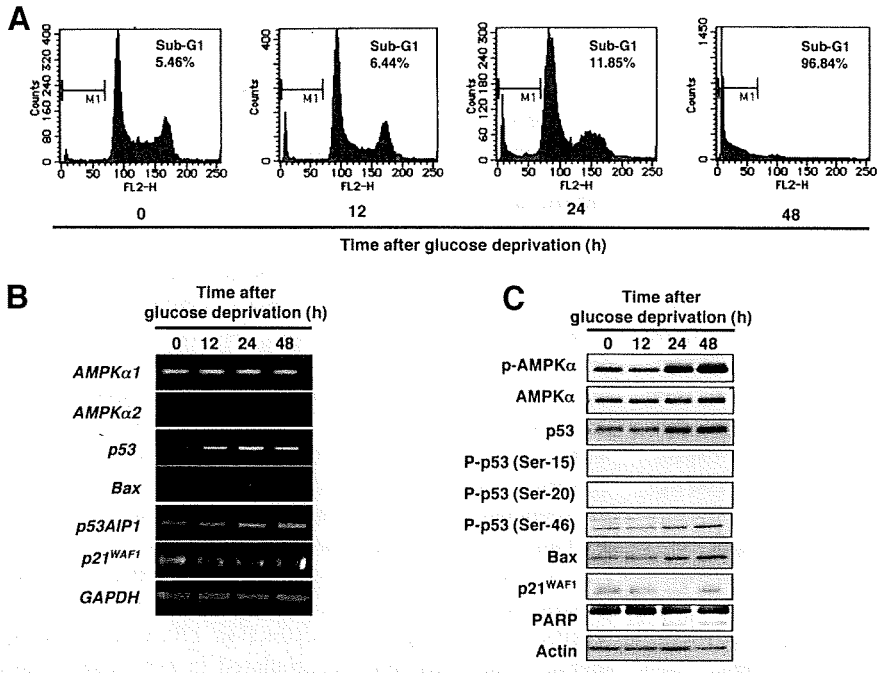

FIGURE 2. **Glucose starvation-mediated apoptotic cell death is associated with a significant induction of p53 *in vitro*.** *A*, FACS analysis. Human osteosarcoma-derived U2OS cells bearing wild-type p53 were maintained in the absence of glucose. At the indicated times after starvation, floating and attached cells were collected, and apoptosis was determined by FACS analysis of DNA fragmentation of propidium iodide-stained nuclei. *B* and *C*, expression of AMPKα and p53 in response to glucose deprivation. Total RNA and whole cell lysates were prepared from U2OS cells maintained in the absence of glucose for the indicated times and subjected to RT-PCR (*B*) and IB (*C*), respectively. For RT-PCR, *GAPDH* was used as an internal control. For IB, expression of actin was used to control equal loading in whole cell lysates.

and we examined their cell cycle distributions by FACS. As shown in Fig. 2*A*, glucose depletion led to a massive apoptotic cell death. RT-PCR analysis revealed that the expression levels of *AMPKα1* and *AMPKα2* remain unchanged (Fig. 2*B*). Unexpectedly, *p53* was transcriptionally induced upon removal of glucose, which was associated with the up-regulation of pro-apoptotic *Bax* and *p53AIP1* (25, 26), although the expression levels of $p21^{WAF1}$ remained almost constant during the glucose deprivation-mediated apoptotic cell death. Immunoblot analysis demonstrated that AMPKα is induced to be phosphorylated following glucose starvation (Fig. 2*C*). In contrast, total amounts of AMPKα remained unchanged even in the absence of glucose. Additionally, glucose deprivation led to an accumulation of p53 as well as an induction of p53 phosphorylation at Ser-46 but not at Ser-15 and Ser-20. As expected, the expression levels of pro-apoptotic Bax but not of $p21^{WAF1}$ increased, and proteolytic cleavage of PARP was detectable in response to glucose deprivation.

Effects of p53 Knockdown on Glucose Deprivation-mediated Apoptotic Cell Death—To ask whether p53 could be involved in apoptotic cell death in response to glucose removal, U2OS cells were transiently transfected with control siRNA or with siRNA against p53. Twenty four hours after transfection, cells were switched into fresh medium lacking glucose. At the indicated time points after glucose starvation, whole cell lysates were prepared and analyzed for the expression levels of p53 by immunoblotting. As shown in Fig. 3*A*, p53 was induced to accumulate in cells transfected with control siRNA, whereas the amounts of p53 were kept at extremely low levels in cells transfected with siRNA against p53. FACS analysis revealed that siRNA-mediated knockdown of p53 strongly reduces the number of cells with sub-G_1 DNA content in response to glucose deprivation as compared with that of control cells (Fig. 3*B*). Similarly, *p53*-deficient human osteosarcoma-derived SAOS-2 cells underwent apoptotic cell death in response to glucose deprivation to a lesser degree, suggesting that p53 contributes at least in part to the induction of apoptotic cell death following glucose depletion.

Because glucose deprivation resulted in the strong induction of AMPKα phosphorylation, we examined the effects of

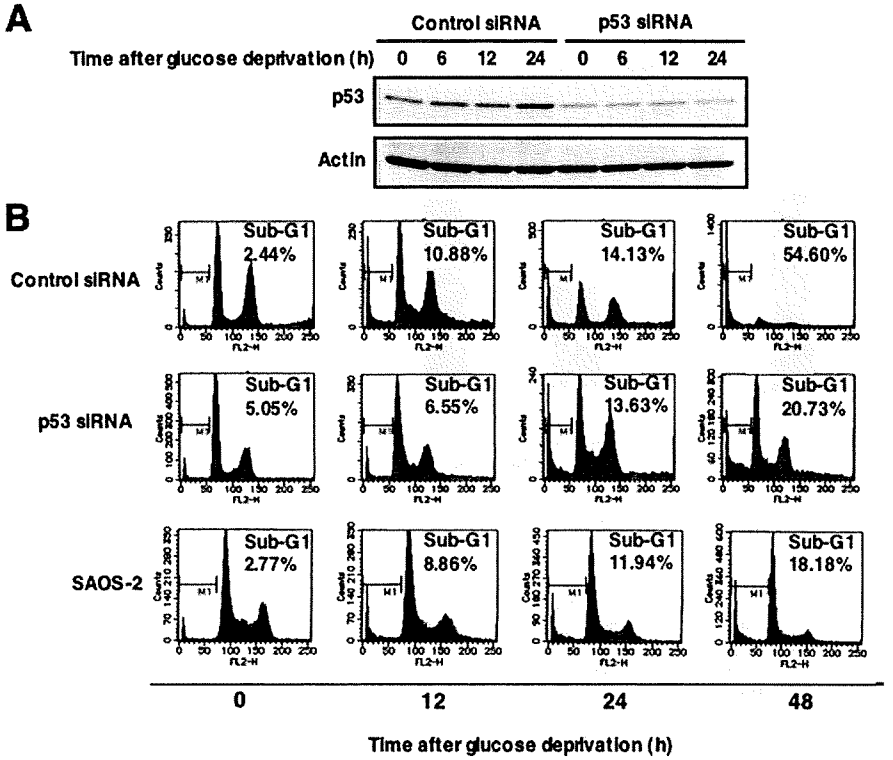

FIGURE 3. **Glucose deprivation-mediated apoptotic cell death is regulated in a p53-dependent manner.** *A*, siRNA-mediated knockdown of p53. U2OS cells were transfected with control siRNA or with siRNA against p53. Twenty-four hours after transfection, cells were transferred into fresh medium without glucose. At the indicated times after starvation, whole cell lysates were prepared and processed for IB with the indicated antibodies. *B*, transfected U2OS cells and *p53*-deficient human osteosarcoma SAOS-2 cells were maintained in the absence of glucose. At the indicated time points, floating and attached cells were harvested and subjected to FACS analysis.

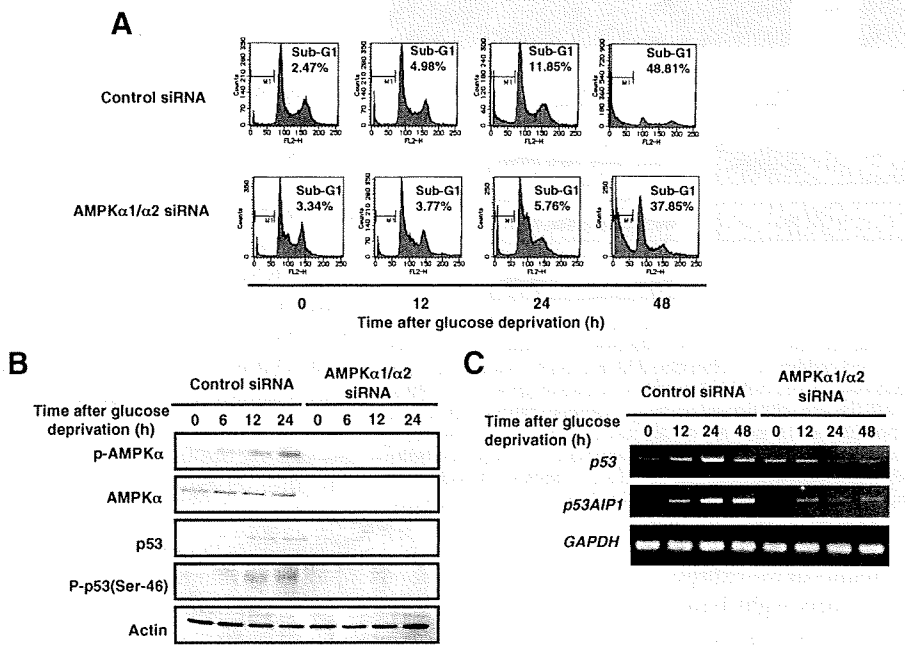

FIGURE 4. **Effects of siRNA-mediated knockdown of AMPKα on apoptotic cell death and p53.** *A*, FACS analysis. U2OS cells were transfected with control siRNA or with siRNAs targeting AMPKα1 plus AMPKα2. Twenty four hours after transfection, cells were transferred into fresh medium without glucose. At the indicated time points after starvation, cells were harvested, and apoptotic cell death was determined by FACS analysis of DNA fragmentation of propidium iodide-stained nuclei. *B* and *C*, effects of AMPKα depletion on p53 in response to glucose removal. U2OS cell were transfected as in *A*. Twenty-four hours after transfection, cells were maintained in the absence of glucose. At the indicated time points after starvation, whole cell lysates and total RNA were prepared and subjected to IB (*B*) and RT-PCR (*C*), respectively.

AMPKα on glucose deprivation-mediated apoptotic cell death. To this end, siRNA-mediated knockdown of AMPKα1 and AMPKα2 was performed. Twenty four hours after transfection, cells were maintained in the absence of glucose. At the indicated time points after glucose starvation, cells were harvested, and their cell cycle distributions were analyzed by FACS. As shown in Fig. 4*A*, siRNA-mediated knockdown remarkably inhibited apoptotic cell death caused by glucose removal relative to control cells. Immunoblot analysis demonstrated that simultaneous knockdown of AMPKα1 and AMPKα2 does not induce the phosphorylation of AMPKα as well as the accumulation of p53 in response to glucose deprivation (Fig. 4*B*). Intriguingly, induction of p53 phosphorylation at Ser-46 was not detectable in cells where AMPKα1 and AMPKα2 were knocked down. Additionally, RT-PCR analysis showed that knockdown of AMPKα1 and AMPKα2 significantly inhibits the transcriptional up-regulation of *p53* as well as *p53 AIP1* (Fig. 4*C*). Under our experimental conditions, these results suggest that AMPKα regulates the glucose deprivation-mediated apoptotic cell death through the induction of p53 at mRNA and protein levels.

AMPKα Has an Ability to Transactivate p53—Although accumulating evidence suggests that p53 is stabilized at a protein level in response to a variety of cellular stresses (19–21), our present results suggest that activation of AMPKα induces the transcriptional activation of *p53*. To address whether the *p53* promoter could respond to AMPKα, we have generated a luciferase reporter construct carrying a 5′-upstream region that encompasses nucleotide sequences from −2000 to +22 relative to the first transcriptional initiation site of the human *p53* gene termed p53-luc (*upper panel* of Fig. 5). U2OS cells were transiently transfected with the constant amount of p53-luc and pRL-TK

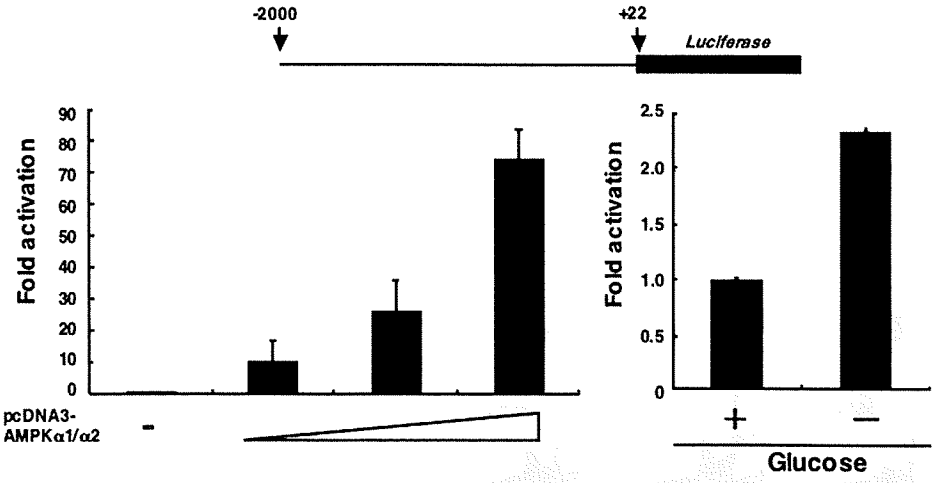

FIGURE 5. **Transcriptional regulation of *p53* by AMPKα.** A schematic drawing of the luciferase reporter construct containing 5′-upstream region of human *p53* gene (termed p53-luc) is shown. The positions relative to the transcriptional initiation site of the *p53* gene (+1) are indicated (*upper panel*). For luciferase reporter assay, U2OS cells were transfected with the constant amount of p53-luc (100 ng) and *Renilla* luciferase reporter plasmid (pRL-TK) (10 ng) together with or without the increasing amounts of the expression plasmids for AMPKα1 plus AMPK α2 (50, 100, or 200 ng). Total amount of plasmid DNA per transfection was kept constant with pcDNA3. Forty-eight hours after transfection, cells were lysed, and their luciferase activities were measured by dual luciferase reporter system. The firefly luminescence signal was normalized based on the *Renilla* luminescence signal. The results were obtained by at least four independent experiments and represent as means ± S.D. (*lower left panel*). Alternatively, U2OS cells were transfected with the constant amount of p53-luc plus pRL-TK. Twenty-four hours after transfection, cells were maintained in the presence or absence of glucose. Forty-eight hours after starvation, cells were lysed, and their luciferase activities were measured (*lower right panel*).

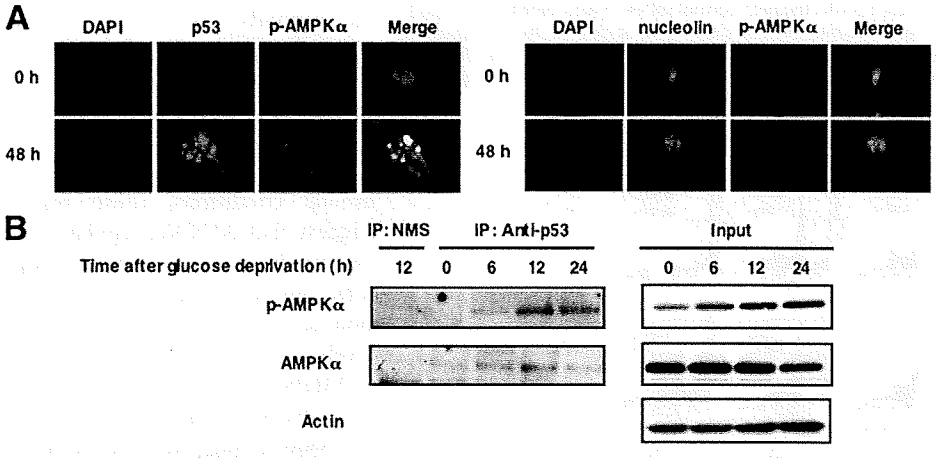

FIGURE 6. **Interaction between AMPKα and p53.** *A*, indirect immunofluorescence staining of p53 and phospho-AMPKα in response to glucose depletion. At the indicated times after glucose deprivation, U2OS cells were fixed, permeabilized, and double-stained for p53 (*green*) and phospho-AMPKα (*red*). Cell nuclei were stained with DAPI (*blue*) (*left panels*). Similarly, U2OS cells were double-stained for nucleolin (*green*) and phospho-AMPKα (*red*). Cell nuclei were stained with DAPI (*blue*) (*right panels*). *B*, immunoprecipitation. U2OS cells were maintained in the absence of glucose. At the indicated times after starvation, whole cell lysates were prepared and immunoprecipitated (*IP*) with normal mouse serum (*NMS*) or with monoclonal anti-p53 antibody followed by IB with polyclonal anti-phospho-AMPKα (*1st panel*) or with polyclonal anti-AMPKα antibody (*2nd panel*). The *right panels* show the expression of phospho-AMPKα (*1st panel*), AMPKα (*2nd panel*), and actin (*3rd panel*) in response to glucose deprivation.

together with or without the increasing amounts of the expression plasmids for AMPKα1 and AMPKα2. Forty eight hours after transfection, cells were lysed, and their luciferase activities were measured. As shown in *lower left panel* of Fig. 5, simultaneous expression of AMPKα1 and AMPKα2 increased the luciferase activities driven by *p53* promoter in a dose-dependent manner. Furthermore, luciferase activities driven by the *p53* promoter were significantly increased in response to glucose starvation (*lower right panel* of Fig. 5). These results were consistent with our present observations showing that p53 is regulated at least in part at a transcriptional level following glucose depletion. However, the precise molecular mechanisms behind the AMPKα-mediated transcriptional activation of *p53* promoter remain unclear. Further studies are necessary to address this issue.

Interaction between AMPKα and p53 in Cells—Next, we examined whether AMPKα could associate with p53 in cells. For this purpose, we performed the indirect immunofluorescence staining experiments. At the indicated times after glucose deprivation, U2OS cells were double-stained with anti-p53 and anti-phospho-AMPKα antibodies. Cell nuclei were stained with DAPI. Merged images clearly showed that p53 co-localizes with phospho-AMPKα within the cell nucleus, and their staining patterns are punctate in response to glucose deprivation (*left panels* of Fig. 6*A*). Because phospho-AMPKα co-localized with nucleolin, which is one of the convenient markers for nucleoli (*right panels* of Fig. 6*A*), it is likely that p53 co-localizes with phospho-AMPKα in nucleoli. Under our experimental conditions, any significant signals were undetectable in the absence of secondary antibody, and glucose deprivation-mediated accumulation of phospho-AMPKα in nucleoli was not observed in cells transfected with siRNA against AMPKα (supplemental Fig. S1). To further confirm the complex formation of p53 with AMPKα, we performed immunoprecipitation experiments. U2OS cells were cultured in the absence of glucose. At the indicated time periods after glucose removal, whole cell lysates were prepared and immunoprecipitated with monoclonal anti-p53 antibody followed by immunoblotting with polyclonal anti-phospho-AMPKα or with polyclonal anti-ANPKα antibody. Under our experimental conditions, phospho-AMPKα and AMPKα were not co-immunoprecipitated with normal mouse serum. As shown in Fig. 6*B*, the anti-p53 immunoprecipitates contained phospho-AMPKα and AMPKα, suggesting that p53 might be associated with both phosphorylated and unphosphorylated forms of AMPKα. Our *in vitro* pulldown assays showed that the radiolabeled AMPKα2

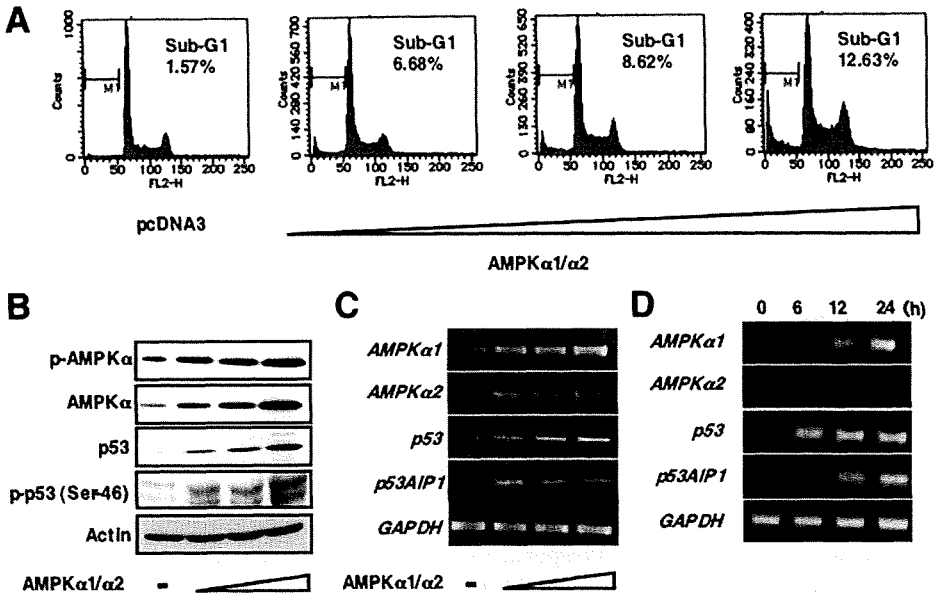

FIGURE 7. **AMPKα has an ability to induce the transcription of *p53* gene and the phosphorylation of p53 at Ser-46.** *A*, AMPKα induces apoptotic cell death. U2OS cells were transfected with the indicated combinations of the expression plasmids. Forty-eight hours after transfection, floating and attached cells were harvested, and the number of cells with sub-G_1 DNA content was measured by FACS. *B* and *C*, AMPKα induces p53. U2OS cells were transiently transfected with or without the increasing amounts of the expression plasmids for AMPKα1 plus AMPKα2. Forty-eight hours after transfection, whole cell lysates and total RNA were prepared and subjected to IB (*B*) and RT-PCR (*C*), respectively. *D*, time course experiments. U2OS cells were transiently co-transfected as in *B*. At the indicated time points after transfection, total RNA was extracted and analyzed for the expression levels of *AMPKα*, *p53*, and *p53 AIP1* by RT-PCR.

but not AMPKα1 is co-immunoprecipitated with the endogenous p53 (supplemental Fig. S2).

Enforced Expression of AMPKα Induces Apoptotic Cell Death in Association with the Up-regulation of p53—To confirm whether AMPKα could promote apoptotic cell death through the induction of p53, U2OS cells were transiently transfected with or without the increasing amounts of the expression plasmids for AMPKα1 and AMPKα2. Forty eight hours after transfection, cells were harvested, and their cell cycle distributions were analyzed by FACS. As shown in Fig. 7*A*, cells underwent apoptotic cell death in a dose-dependent manner. Immunoblot analysis demonstrated that the exogenously expressed AMPKα is phosphorylated in a dose-dependent fashion (Fig. 7*B*). As expected, levels of total p53 and its phosphorylation at Ser-46 were elevated in the presence of exogenously expressed AMPKα1 and AMPKα2. Consistent with our present results, enforced expression of AMPKα1 and AMPKα2 resulted in the transcriptional up-regulation of *p53* as well as pro-apoptotic *p53 AIP1* (Fig. 7*C*). In addition, simultaneous expression of AMPKα1 and AMPKα2 led to an induction of *p53* and *p53 AIP1* in a time-dependent manner (Fig. 7*D*). Taken together, our present findings suggest that AMPK-mediated induction of p53 plays an important role in the regulation of cell fate determination in response to glucose deprivation.

DISCUSSION

Recently, it has been shown that, under low glucose conditions, AMPK-dependent activation of tumor suppressor p53 causes cell cycle arrest, suggesting that p53 might act as a metabolic sensor in response to glucose limitation (22). According to their results, AMPK-dependent phosphorylation of p53 at Ser-15 plays an essential role in mediating the effects of activated AMPK on p53-dependent cell cycle arrest. In contrast, glucose depletion led to apoptotic cell death through the activation of pro-apoptotic Bax (27). In this study, we have found that glucose deprivation enhances the phosphorylation of AMPKα and induces p53-dependent apoptotic cell death *in vivo* and *in vitro*. Intriguingly, glucose depletion-mediated apoptotic cell death was associated with a significant transcriptional up-regulation of *p53* and specific induction of p53 phosphorylation at Ser-46.

In response to various cellular stresses such as DNA damage, p53 is extensively phosphorylated at several amino acid residues, including Ser-15, Ser-20, and Ser-46 (21). Induction of cell cycle arrest and apoptotic cell death has been considered to be the most important biological functions of p53 in cells exposed to various cellular stresses (19–21); however, the precise molecular mechanisms responsible for the choice between p53-dependent cell cycle arrest and apoptotic cell death in response to cellular stresses have been elusive. Previously, Oda *et al.* (25) found an important clue to understand this issue. According to their results, p53 was extensively phosphorylated at Ser-46 following severe DNA damage, and thereby cells with damaged DNA underwent apoptotic cell death. Thus, DNA damage-induced phosphorylation of p53 at Ser-46 might trigger the p53-dependent apoptotic program mediated by pro-apoptotic *p53 AIP1*. *p53 AIP1*, which is localized in mitochondria, is one of direct transcriptional targets of p53 and has an ability to down-regulate mitochondrial membrane potential and thereby release cytochrome *c* from the mitochondria to the cytoplasm (25, 26). Therefore, it is likely that the stress-induced phosphorylation of p53 at Ser-46 is one of the critical events for commitment of cell fate into apoptotic cell death. Based on our present results, metabolic stress elicited by glucose deprivation promoted apoptotic cell death in association with a significant phosphorylation of AMPKα as well as p53 at Ser-46 but not at Ser-15 and Ser-20. As expected, phosphorylation of p53 at Ser-46 was significantly associated with the transcriptional up-regulation of pro-apoptotic *Bax* and *p53 AIP1*. In support of these results, siRNA-mediated knockdown of the endogenous AMPKα markedly inhibited the glucose depletion-mediated apoptotic cell death and phosphorylation of p53 at Ser-46 as well as the transcriptional up-regulation of *p53 AIP1*. Indeed, enforced expression of AMPKα promoted apoptotic cell death and p53 phosphorylation at Ser-46 in association with the transcriptional activation of *p53 AIP1*. Collectively, our present

results suggest that the activation of the AMPK complex is required for the metabolic stress-induced phosphorylation of p53 at Ser-46, thereby inducing apoptotic cell death. As described (28–30), HIPK2 (homeodomain-interacting protein kinase-2) associates with p53 and mediates ionizing radiation-induced p53 phosphorylation at Ser-46. In addition to HIPK2, Yoshida *et al.* (31) found that protein kinase Cδ mediates phosphorylation of p53 at Ser-46 in response to genotoxic stress, indicating that protein kinase Cδ is a novel candidate for Ser-46 kinase.

Another new finding of this study was that glucose deprivation-mediated accumulation of p53 might be attributed at least in part to the transcriptional up-regulation of *p53*, and AMPK complex might play an important role in the transcriptional regulation of *p53*. Accumulating evidence strongly suggests that p53 is induced to accumulate through the post-translational modifications such as phosphorylation and acetylation in response to a variety of cellular stresses (19–21). On the other hand, the regulatory mechanisms of *p53* gene transcription have been poorly understood. Previously, Reich and Levine (32) described that *p53* is transcriptionally regulated in response to mitogen stimulation as well as serum starvation. Noda *et al.* (33) identified the promoter element termed PE21 at a nucleotide position from −79 to −60 (relative to the first transcriptional initiation site) within the *p53* promoter region responsible for *p53* gene basal expression and ultraviolet response. In addition, it has been shown that homeobox protein HOXA5 has an ability to transactivate the *p53* gene (34, 35). It is worth noting that there exists a putative p53-responsive element within the *p53* promoter region, thereby forming a novel positive feedback loop regulating p53 expression (36). According to our present results, siRNA-mediated knockdown of the endogenous AMPKα significantly inhibited the transcriptional induction of *p53* in response to glucose deprivation. Consistent with these observations, glucose depletion enhanced the promoter activity of *p53* as examined by luciferase reporter analysis. Furthermore, enforced expression of AMPKα resulted in a dramatic increase in luciferase activities driven by the *p53* promoter in the absence of metabolic stress. Because the AMPK complex is involved in the regulation of gene expression (5), it is possible that the activated form of AMPK complex might induce the transcription of *p53* through as yet unknown direct or indirect mechanisms. Further studies are required to address this issue.

Immunoprecipitation experiments indicated that p53 is associated with both unphosphorylated and phosphorylated forms of AMPKα during glucose deprivation-mediated apoptosis. Considering that glucose depletion-mediated phosphorylation of AMPKα is significantly associated with the up-regulation of p53, it is likely that phosphorylated forms of AMPKα might contribute to glucose starvation-mediated induction of p53 through the interaction with it. Our indirect immunofluorescence staining experiments clearly demonstrated that, upon glucose starvation, phosphorylated forms of AMPKα co-localize with p53 within the nucleolus, a subnuclear compartment that is a site of ribosomal assembly (37). In addition to the production of ribosomes, it has been postulated that the nucleolus might be involved in numerous cellular processes, including cell cycle control, DNA damage repair, and tRNA processing (38). Recently, Karni-Schmidt *et al.* (39) reported that nuclear localization signal I and the extreme COOH-terminal region of p53 are required for its nucleolar distribution. Although the functional consequences of the nucleolar localization of p53 are largely unknown, Wesierska-Gadek *et al.* (40) reported that the nucleolar distribution of p53 might contribute to its reactivation in response to genotoxic stress caused by cisplatin treatment. Thus, it is possible that the nucleolus might provide an important subnuclear locale for p53 function under specific conditions. According to our *in vitro* pulldown assay, AMPKα2 but not AMPKα1 was co-immunoprecipitated with endogenous p53. AMPK is a heterotrimeric protein kinase consisting of α, β, and γ subunits. In mammalian cells, each subunit exists in different isoforms, which might give rise to 12 distinct heterotrimeric isoform-subunit combinations. Recently, it has been shown that two wild-type AMPK complexes containing AMPKα1 or AMPKα2 display similar catalytic activities and equal response to AMP (41). Based on our present results, it is likely that AMPKα2-containing AMPK complexes might have a distinct role in the regulation of apoptotic cell death through the functional interaction with p53, although further experiments are required to address this issue.

Acknowledgment—We thank Y. Nakamura for technical assistance.

REFERENCES

1. Beg, G. H., Allmann, D. W., and Gibson, D. M. (1973) *Biochem. Biophys. Res. Commun.* **54,** 1362–1369
2. Carlson, C. A., and Kim, K. H. (1973) *J. Biol. Chem.* **248,** 378–380
3. Rutter, G. A., Da Silva Xavier, G., and Leclerc, I. (2003) *Biochem. J.* **375,** 1–16
4. Carling, D. (2004) *Trends Biochem. Sci.* **29,** 18–24
5. Hardie, D. G. (2004) *J. Cell Sci.* **117,** 5479–5487
6. Hardie, D. G. (2003) *Endocrinology,* **144,** 5179–5183
7. Xing, Y., Musi, N., Fujii, N., Zou, L., Luptak, I., Hirshman, M. F., Goodyear, L. J., and Tian, R. (2003) *J. Biol. Chem.* **278,** 28372–28377
8. Hawley, S. A., Boudeau, J., Reid, J. L., Mustard, K. J., Udd, L., Makela, T. P., Allesi, D. R., and Hardie, D. G. (2003) *J. Biol.* **2,** 28
9. Woods, A., Johnstone, S. R., Dickerson, K., Leiper, F. C., Fryer, L. G., Neumann, D., Schlattner, U., Wallimann, T., Carlson, M., and Carling, D. (2003) *Curr. Biol.* **13,** 2004–2008
10. Shaw, R. J., Bardeesy, N., Manning, B. D., Lopez, L., Kosmatka, M., DePinho, R. A., and Cantley, L. C. (2004) *Cancer Cell* **6,** 91–99
11. Hardie, D. G., Carling, D., and Carlson, M. (1998) *Annu. Rev. Biochem.* **67,** 821–855
12. Vogelstein, B., Lane, D., and Levine, A. J. (2000) *Nature* **408,** 307–310
13. Caron de Fromentel, C., and Soussi, T. (1992) *Genes Chromosomes Cancer* **4,** 1–15
14. Greenblatt, M. S., Bennett, W. P., Hollstein, M., and Harris, C. C. (1994) *Cancer Res.* **54,** 4855–4878
15. Chao, C., Hergenhahn, M., Kaeser, M. D., Wu, Z., Saito, S., Iggo, R., Hollstein, M., Appella, E., and Xu, Y. (2003) *J. Biol. Chem.* **278,** 41028–41033
16. Donehower, L. A., Harvey, M., Slagle, B. L., McArthur, M. J., Montgomery, C. A., Jr., Butel, J. S., and Bradley, A. (1992) *Nature* **356,** 215–221
17. Haupt, Y., Maya, R., Kazaz, A., and Oren, M. (1997) *Nature* **387,** 296–299
18. Kubbutat, M. H., Jones, S. N., and Vousden, K. (1997) *Nature* **387,** 299–303
19. Prives, C., and Hall, P. A. (1999) *J. Pathol.* **187,** 112–126
20. Sionov, R. V., and Haupt, Y. (1999) *Oncogene* **18,** 6145–6157
21. Vousden, K. H., and Lu, X. (2002) *Nat. Rev. Cancer* **2,** 594–604
22. Jones, R. G., Plas, D. R., Kubek, S., Buzzai, M., Mu, J., Xu, Y., Birnbaum,

M. J., and Thompson, C. B. (2005) *Mol. Cell* **18,** 283–293
23. Imamura, K., Ogura, T., Kishimoto, A., Kaminishi, M., and Esumi, H. (2001) *Biochem. Biophys. Res. Commun.* **287,** 562–567
24. Stefanelli, C., Stanic, I., Bonavita, F., Flamigni, F., Pignatti, C., Guarnieri, C., and Caldarera, C. M. (1998) *Biochem. Biophys. Res. Commun.* **243,** 821–826
25. Oda, K., Arakawa, H., Tanaka, T., Matsuda, K., Tanikawa, C., Mori, T., Nishimori, H., Tamai, K., Tokino, T., Nakamura, Y., and Taya, Y. (2000) *Cell* **102,** 849–862
26. Matsuda, K., Yoshida, K., Taya, Y., Nakamura, K., Nakamura, Y., and Arakawa, H. (2002) *Cancer Res.* **62,** 2883–2889
27. Rathmell, J. C., Fox, C. J., Plas, D. R., Hammerman, P. S., Cinalli, R. M., and Thompson, C. B. (2003) *Mol. Cell. Biol.* **23,** 7315–7328
28. Hofmann, T. G., Moller, A., Sirma, H., Zentgraf, H., Taya, Y., Droge, W., Will, H., and Schmitz, M. L. (2002) *Nat. Cell Biol.* **4,** 1–10
29. D'Orazi, G., Cecchinelli, B., Bruno, T., Manni, I., Higashimoto, Y., Saito, S., Gostissa, M., Coen, S., Marchetti, A., Del Sal, G., Piaggio, G., Fanciulli, M., Appella, E., and Soddu, S. (2002) *Nat. Cell Biol.* **4,** 11–19
30. Dauth, I., Kruger, J., and Hofmann, T. G. (2007) *Cancer Res.* **67,** 2274–2279
31. Yoshida, K., Liu, H., and Miki, Y. (2006) *J. Biol. Chem.* **281,** 5734–5740
32. Reich, N. C., and Levine, A. J. (1984) *Nature* **308,** 199–201
33. Noda, A., Toma-Aiba, Y., and Fujiwara, Y. (2000) *Oncogene* **19,** 21–31
34. Raman, V., Martensen, S. A., Reisman, D., Evron, E., Odenward, W. F., Jaffee, E., Marks, J., and Sukumar, S. (2000) *Nature* **405,** 974–978
35. Raman, V., Tamori, A., Vali, M., Zeller, K., Korz, D., and Sukumar, S. (2000) *J. Biol. Chem.* **275,** 26551–26555
36. Wang, S., and El-Deiry, W. S. (2006) *Cancer Res.* **66,** 6982–6989
37. Garcia, S. N., and Pillus, L. (1999) *Cell* **97,** 825–828
38. Mekhail, K., Khacho, M., Carrigan, A., Hache, R. R., Gunaratnam, L., and Lee, S. (2005) *J. Cell Biol.* **170,** 733–744
39. Karni-Schmidt, O., Friendler, A., Zupnick, A., McKinney, K., Mattia, M., Beckerman, R., Bouvet, P., Sheetz, M., Fersht, A., and Prives, C. (2007) *Oncogene* **26,** 3878–3891
40. Wesierska-Gadek, J., Schloffer, D., Kotata, V., and Horky, M. (2002) *Int. J. Cancer* **101,** 128–136
41. Suter, M., Riek, U., Tuerk, R., Schlattner, U., Wallimann, T., and Neumann, D. (2006) *J. Biol. Chem.* **281,** 32207–32216

Oncogene (2008) 27, 3700–3709

www.nature.com/onc

ORIGINAL ARTICLE

A novel HECT-type E3 ubiquitin protein ligase NEDL1 enhances the p53-mediated apoptotic cell death in its catalytic activity-independent manner

Y Li[1,2,3], T Ozaki[1,3], H Kikuchi[1], H Yamamoto[1], M Ohira[1] and A Nakagawara[1]

[1]*Division of Biochemistry, Chiba Cancer Center Research Institute, Nitona, Chuou-Ku, Chiba, Japan and* [2]*Production Technology Development Center, the Furukawa Electric Co., Ltd., 6 Yawata-Kaigandori, Ichihara, Japan*

NEDL1 (NEDD4-like ubiquitin protein ligase-1) is a newly identified HECT-type E3 ubiquitin protein ligase highly expressed in favorable neuroblastomas as compared with unfavorable ones. In this study, we found that NEDL1 cooperates with p53 to induce apoptosis. During cisplatin (CDDP)-mediated apoptosis in neuroblastoma SH-SY5Y cells, p53 was induced to accumulate in association with an increase in expression levels of NEDL1. Enforced expression of NEDL1 resulted in a decrease in number of G418-resistant colonies in SH-SY5Y and U2OS cells bearing wild-type *p53*, whereas NEDL1 had undetectable effect on *p53*-deficient H1299 and SAOS-2 cells. Similarly, enforced expression of NEDL1 increased number of U2OS cells with sub-G1 DNA content. Co-immunoprecipitation and *in vitro* binding assays revealed that NEDL1 binds to the COOH-terminal region of p53. Luciferase reporter assay showed that NEDL1 has an ability to enhance the transcriptional activity of p53. Small interfering RNA-mediated knockdown of the endogenous NEDL1 conferred the resistance of U2OS cells to adriamycin. It is noteworthy that NEDL1 enhanced pro-apoptotic activity of p53 in its catalytic activity-independent manner. Taken together, our present findings suggest that functional interaction of NEDL1 with p53 might contribute to the induction of apoptosis in cancerous cells bearing wild-type *p53*.

Oncogene (2008) **27**, 3700–3709; doi:10.1038/sj.onc.1211032; published online 28 January 2008

Keywords: apoptosis; cisplatin; DNA damage; HECT-type E3 ubiquitin ligase; NEDL1; p53

Introduction

NEDL1 (NEDD4-like ubiquitin protein ligase-1), which has been identified as a novel gene expressed significantly at high levels in favorable neuroblastomas relative to unfavorable ones, encodes HECT-type E3 ubiquitin ligase and is detected specifically in human neuronal tissues (Miyazaki *et al.*, 2004), suggesting that NEDL1 might be involved in the regulation of the spontaneous regression of favorable neuroblastomas caused by apoptosis and/or neuronal differentiation. According to our previous findings, NEDL1 ubiquitinated mutant forms of SOD1 (superoxide dismutase-1) as well as Dvl-1 (Dishevelled-1), thereby promoting their proteasome-dependent degradation (Miyazaki *et al.*, 2004). SOD1 mutations have been detected in a certain subset of patients with familial amyotrophic lateral sclerosis, which is one of the fatal neurological diseases in human, and mutant SOD1 aggregates to form insoluble macromolecular protein complexes in motor neurons and astrocytes (Cluskey and Ramsden, 2001), suggesting that the accumulation of misfolded proteins generates cellular stresses to induce neuronal cell death. However, the precise molecular mechanisms behind the possible contribution of NEDL1 to apoptosis in motor neurons remain elusive.

As described previously (Gonzalez de Aguilar *et al.*, 2000), pro-apoptotic Bax, which is one of the direct targets of tumor suppressor p53 (Roos and Kaina, 2006), accumulated in central nervous system regions in patients with amyotrophic lateral sclerosis. In support of this notion, p53 was induced in central nervous system regions in patients and also in model mice with amyotrophic lateral sclerosis (Martin, 2000), indicating that p53-mediated pro-apoptotic pathway plays an important role in the regulation of neuronal apoptosis. p53 is a nuclear transcription factor that induces cell cycle arrest and/or apoptosis. Under normal conditions, p53 is kept at extremely low level. The expression of p53 is regulated largely at protein level. For example, E3 ubiquitin ligase MDM2 inhibits transactivation activity of p53 and also promotes its ubiquitination-mediated proteasomal degradation (Vousden and Lu, 2002). In response to genotoxic stresses, p53 is induced to be converted from the latent form to the active one through the post-translational modifications such as phosphorylation and acetylation, and thereby transactivating its direct target genes implicated in cell cycle arrest and/or apoptosis including $p21^{WAF1}$, *MDM2*, *Bax*, *Puma*, *Noxa* and *p53AIP1* (Vousden and Lu, 2002). Accumulating evidence strongly suggests that its transactivation

Correspondence: Dr A Nakagawara, Division of Biochemistry, Chiba Cancer Center Research Institute, 666-2 Nitona, Chuou-Ku, Chiba 260-8717, Japan.
E-mail: akiranak@chiba-cc.jp
[3]These authors contributed equally to this work.
Received 16 May 2007; revised 26 November 2007; accepted 10 December 2007; published online 28 January 2008

activity is tightly linked to its pro-apoptotic function (Pietenpol *et al.*, 1994). Consistent with this notion, majority of loss-of-function mutations of p53 in a variety of primary human tumors is detected within its DNA-binding domain (Hollstein *et al.*, 1991; Levine *et al.*, 1994) and *p53*-deficient mice developed spontaneous tumors (Donehower *et al.*, 1992).

In the present study, we found that NEDL1 binds to the COOH-terminal region of p53 and enhances its transcriptional activity as well as pro-apoptotic function in its catalytic activity-independent manner. Our present findings suggest that NEDL1 plays a pivotal role in the induction of apoptosis in cancerous cells bearing wild-type *p53* through the interaction with p53 and also might provide a novel insight into understanding neuronal dysfunction.

Results

NEDL1 has a pro-apoptotic function

As described previously (Miyazaki *et al.*, 2004), we cloned a novel gene termed *NEDL1* from the oligo-capping cDNA libraries prepared from a mixture of fresh primary neuroblastoma tissues that underwent spontaneous regression (Nakagawara and Ohira, 2004). *NEDL1* was highly expressed in favorable neuroblastomas as compared with unfavorable ones and significantly associated with better prognosis in neuroblastoma (Supplementary Figure S1). To examine the expression levels of NEDL1 in response to DNA damage, human neuroblastoma SH-SY5Y cells bearing wild-type *p53* were exposed to 20 μM of cisplatin (CDDP). At the indicated time periods, cells were subjected to terminal deoxynucleotidyl transferase-mediated dUTP-biotin nick end labeling (TUNEL) staining. As shown in Figure 1a, SH-SY5Y cells underwent apoptosis in a time-dependent manner. We then analysed the expression patterns of NEDL1 and p53 in response to CDDP. As shown in Figures 1b and c, p53 was induced to accumulate at protein level but not at mRNA level and CDDP treatment promoted phosphorylation of p53 at Ser-15 in association with a significant upregulation of various p53 target genes such as $p21^{WAF1}$, *Bax* and *Noxa*. It is noteworthy that NEDL1 increased at both mRNA and protein levels in SH-SY5Y cells exposed to CDDP in a time-dependent manner. *NEDL1* was also upregulated in *p53*-deficient human lung carcinoma H1299 cells in response to CDDP (Figure 1d), indicating that *NEDL1* might not be a direct target of p53. Since a correlation between expression levels of NEDL1 and p53 was observed in SH-SY5Y cells treated with CDDP, it is likely that there could exist a functional interaction between them during DNA damage-mediated apoptotic response.

To confirm this notion, we performed colony formation assay. *p53*-proficient SH-SY5Y, human osteosarcoma U2OS, *p53*-deficient human lung carcinoma H1299 and human osteosarcoma SAOS-2 cells were transfected

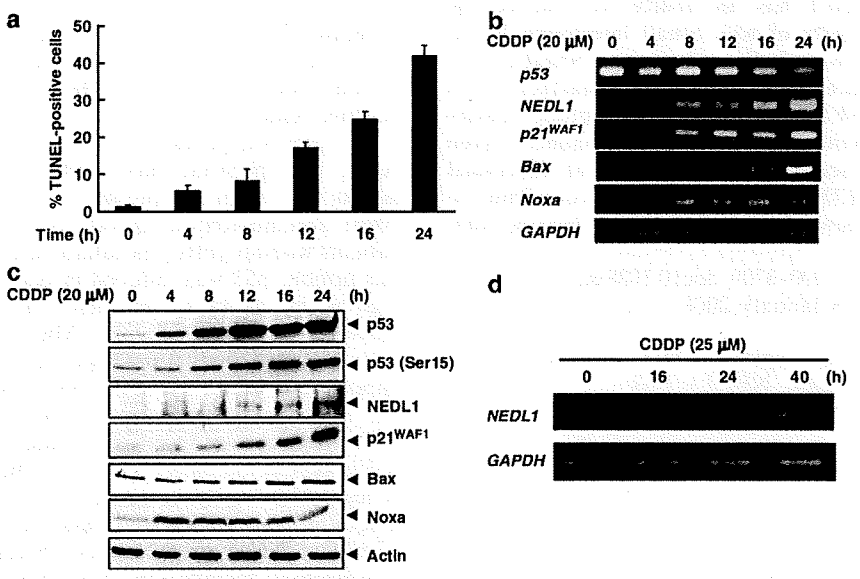

Figure 1 NEDL1 is induced to accumulate in response to CDDP. (a) CDDP-mediated apoptosis. SH-SY5Y cells were treated with CDDP (20 μM). Cells were then stained with an *in situ* cell death detection kit followed by mounting with 4′,6-diamidino-2-phenylindole-containing mounting medium. The number of TUNEL-positive cells was scored. Results were expressed as means ± s.d. of three independent experiments. (b and c) Expressions of NEDL1 and p53 in response to CDDP. Total RNA and cell lysates were prepared from SH-SY5Y cells exposed to CDDP for the indicated time periods and subjected to RT PCR (b) and immunoblotting (c), respectively. (d) *NEDL1* is induced in *p53*-deficient H1299 cells exposed to CDDP. H1299 cells were treated with 25 μM of CDDP. At the indicated time points, total RNA was prepared and analysed for the expression levels of *NEDL1* by RT PCR. *GAPDH* was used as an internal control. CDDP, cisplatin; GAPDH, glyceraldehyde-3-phosphate dehydrogenase; NEDL1, NEDD4-like ubiquitin protein ligase-1; RT PCR, reverse transcription PCR; TUNEL, terminal deoxynucleotidyl transferase-mediated dUTP-biotin nick end labeling.

with empty plasmid or with expression plasmid for NEDL1. Following 2 weeks of selection with G418, drug-resistant colonies were stained and photographed. As shown in Figures 2a and b, enforced expression of NEDL1 caused a significant decrease in the number of drug-resistant colonies in *p53*-proficient SH-SY5Y and U2OS cells relative to control cells, whereas NEDL1 had undetectable effects on *p53*-deficient H1299 and SAOS-2 cells, indicating that NEDL1 induces cell cycle arrest and/or apoptosis in cells carrying wild-type *p53*.

To address whether NEDL1 could cooperate with p53 to induce cell cycle arrest and/or apoptosis, we checked NEDL1-mediated proteolytic cleavage of caspase-3. For this purpose, expression plasmid for NEDL1 was introduced into the indicated cells. As shown in Figure 3a, NEDL1-mediated proteolytic cleavage of caspase-3 was detectable in SH-SY5Y and U2OS cells, but not in H1299 and SAOS-2 cells. Furthermore, enforced expression of NEDL1 resulted in an increase in the number of U2OS cells with sub-G1 DNA content (Figure 3b), whereas NEDL1 had negligible effects on SAOS-2 cells (Figure 3c). Since U2OS cells expressed wild-type p53, these findings suggest that NEDL1 induces apoptosis in a p53-dependent manner.

Interaction between NEDL1 and p53

To determine whether NEDL1 could interact with p53, COS7 cells were transfected with NEDL1 expression plasmid. As shown in Figure 4a, the anti-NEDL1 immunoprecipitates contained endogenous p53. To further confirm this issue, cell lysates prepared from U2OS cells exposed to CDDP were immunoprecipitated with normal rabbit serum or with anti-NEDL1 antibody and analysed by immunoblotting with anti-p53 antibody. As shown in Figure 4b, the anti-NEDL1 immunoprecipitates contained endogenous p53, suggesting that NEDL1 associates with endogenous p53 in cells. In contrast to wild-type p53, mutant form of p53 was not co-immunoprecipitated with NEDL1 (Figure 4c). To identify the region(s) of p53 responsible for the interaction with NEDL1, we performed *in vitro* pull-down assay using the indicated radio-labeled p53 deletion mutants. As clearly shown in Figure 4d, full-length p53, p53(1–353) and p53(102–393) were co-immunoprecipitated with NEDL1, whereas remaining p53 deletion mutants including p53(1–292) and p53(1–102) were not. Under our experimental conditions, other p53 family members such as p73 and p63 failed to be co-immunoprecipitated with NEDL1 (data not shown). These results suggest that NEDL1 specifically interacts with COOH-terminal region of p53 (amino-acid residues 293–353) and might modulate p53 function.

NEDL1 enhances the transcriptional activity of p53

Next, we sought to examine a possible effect of NEDL1 on the transcriptional activity of p53. H1299 cells were co-transfected with a constant amount of p53 expression plasmid, together with p53-responsive $p21^{WAF1}$ or *Bax* luciferase reporter construct in the presence or absence of increasing amounts of NEDL1 expression plasmid. As shown in Figures 5a and b, enforced expression of NEDL1 enhanced p53-mediated transactivation toward $p21^{WAF1}$ and *Bax* promoters in a dose-dependent manner. Similarly, luciferase activities driven by $p21^{WAF1}$ promoter were increased by NEDL1 in U2OS cells (Figure 5c). In support of these results, reverse transcription–polymerase chain reaction (RT–PCR) analysis showed that enforced expression of NEDL1 led to a significant increase in expression levels of endogenous $p21^{WAF1}$ and *Noxa* induced by exogenously

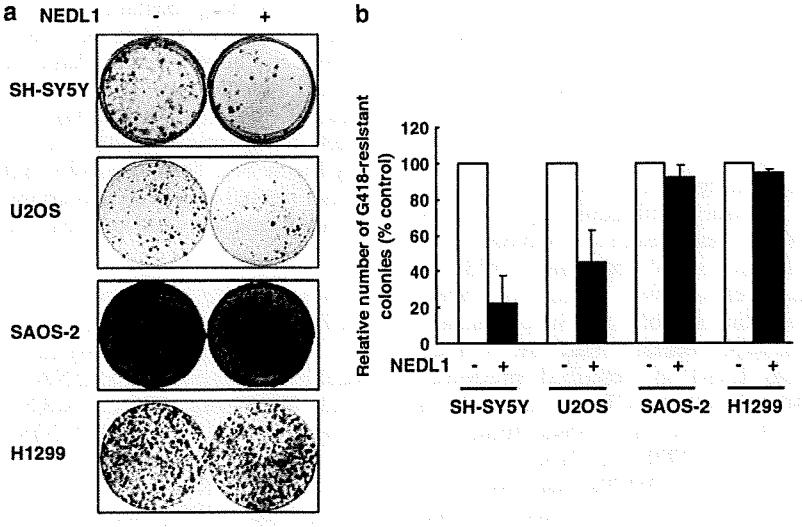

Figure 2 NEDL1 exerts its growth-suppressive and/or pro-apoptotic activity in cancerous cells bearing wild-type *p53*. (**a**) SH-SY5Y cells and U2OS cells harboring wild-type *p53* as well as *p53*-deficient H1299 cells and SAOS-2 cells were transfected with 2.0 μg of empty plasmid (pcDNA3) or with 2.0 μg of expression plasmid for NEDL1. Forty-eight hours after transfection, cells were transferred to fresh medium containing G418 (400 μg ml^{-1}). Two weeks after selection, drug-resistant colonies were stained with Giemsa's solution and photographed. (**b**) Average number of drug-resistant colonies in each transfection relative to pcDNA3 empty plasmid control (set at 100%). Results were expressed as means ± s.d. of three independent experiments. NEDL1, NEDD4-like ubiquitin protein ligase-1.

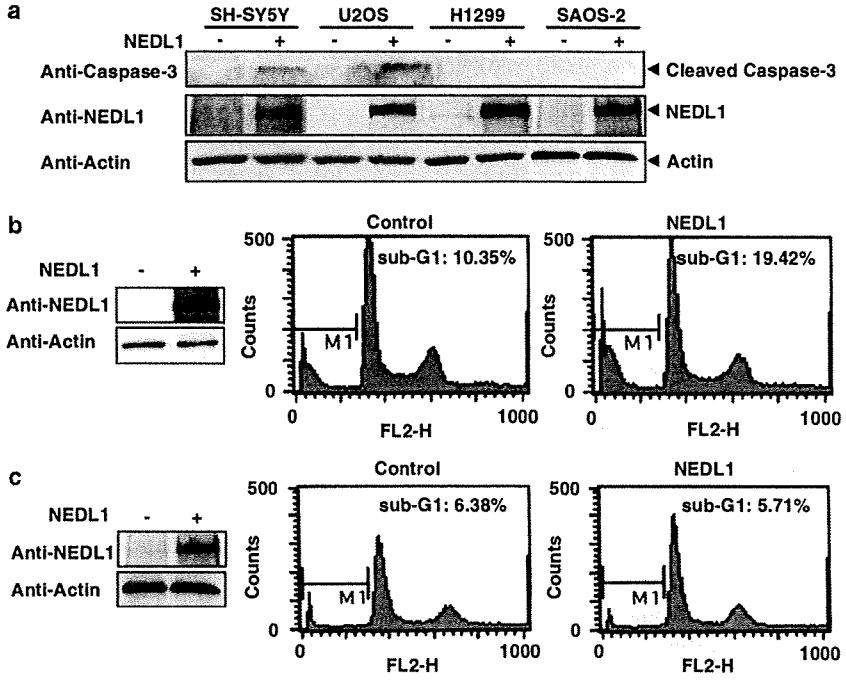

Figure 3 NEDL1 has a pro-apoptotic activity in cells bearing wild-type *p53*. (a) Cleavage of caspase-3. Expression plasmid encoding NEDL1 or empty plasmid was transfected into the indicated cells. Forty-eight hours after transfection, cell lysates were prepared and processed for immunoblotting with the indicated antibodies. (b and c) FACS analysis. U2OS (b) and SAOS-2 (c) cells were transfected with empty plasmid or with expression plasmid for NEDL1. Forty-eight hours after transfection, expression levels of NEDL1 were examined by immunoblotting (left panels) and number of cells with sub-G1 DNA content was analysed by FACS (right panels). NEDL1, NEDD4-like ubiquitin protein ligase-1.

expressed p53 (Figure 5d). Furthermore, chromatin immunoprecipitation (ChIP) assay demonstrated that NEDL1 has an ability to increase the amounts of exogenous and endogenous p53 recruited onto $p21^{WAF1}$ promoter region, whereas NEDL1 alone is not recruited onto $p21^{WAF1}$ promoter region (Figure 5e), indicating that NEDL1 might cooperate with p53 to directly induce the transcription of p53 target genes.

NEDL1 enhanced the pro-apoptotic activity of p53 independent of its ubiquitin ligase activity

Since NEDL1 has an intrinsic E3 ubiquitin ligase activity (Miyazaki *et al.*, 2004), these results prompted us to examine whether NEDL1 could ubiquitinate p53. In spite of our extensive efforts, we could not detect NEDL1-mediated ubiquitination of p53 (Supplementary Figure S2). Under our experimental conditions, NEDL1 efficiently ubiquitinated Dvl-1 as described previously (Miyazaki *et al.*, 2004), whereas HECT(−) mutant failed to ubiquitinate Dvl-1. To extend these observations, we examined a possible effect of NEDL1 catalytic activity on pro-apoptotic function of p53. H1299 cells were co-transfected with a constant amount of expression plasmid for p53 together with or without increasing amounts of wild-type NEDL1 or mutant form of NEDL1 lacking HECT domain termed HECT(−) (Figure 6a). Following 2 weeks of selection with G418 (400 μg ml^{-1}), drug-resistant colonies were stained with Giemsa's solution. Enforced expression of p53 decreased the number of drug-resistant colonies as compared with that in control cells (Figure 6b). As expected, coexpression of p53 plus wild-type NEDL1 or HECT(−) mutant led to a dramatic decrease in the number of drug-resistant colonies in a dose-dependent manner relative to that in cells expressing p53 alone. *In vitro* pull-down assay demonstrated that HECT(−) mutant, but not CW linker, retains an ability to interact with p53 (Figure 6c). In addition, CW linker had negligible effects on the transcriptional activity of p53 (Supplementary Figure S3). Thus, it is likely that NEDL1 enhances the transcriptional as well as pro-apoptotic function of p53 in its catalytic activity-independent manner.

siRNA-mediated knockdown of endogenous NEDL1 confers resistance of U2OS cells to adriamycin

To address the physiological role of endogenous NEDL1 in response to DNA damage, we designed small interfering RNAs (siRNAs) against NEDL1 termed nos. 1, 2, 3 and 4. U2OS cells were transfected with the indicated siRNAs. As shown in Figure 7a, nos. 2, 3 and 4 siRNAs successfully knocked down the endogenous *NEDL1*. We then used nos. 2 and 4 siRNAs for further experiments.

To examine the possible effect of siRNA targeting NEDL1 on the sensitivity to adriamycin (ADR), U2OS cells were transfected with control siRNA, no. 2 or 4 siRNA. Twenty-four hours after transfection, cells were

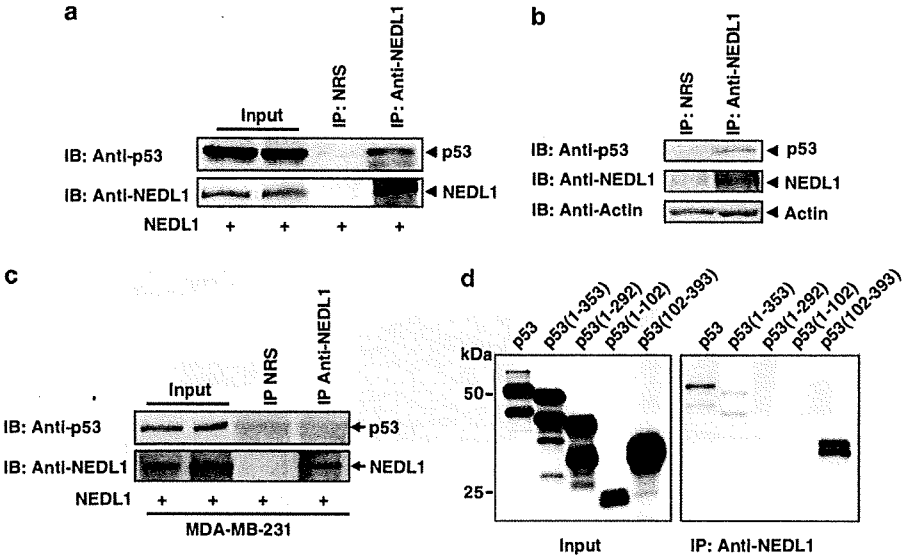

Figure 4 Interaction between NEDL1 and p53. (**a**) Immunoprecipitation. COS7 cells were transfected with NEDL1 expression plasmid. Forty-eight hours after transfection, cell lysates were prepared and immunoprecipitated with NRS or with polyclonal anti-NEDL1 antibody. Immunoprecipitates were analysed by immunoblotting with the indicated antibodies. Ten percentage of inputs were also loaded (input). (**b**) Endogenous interaction between NEDL1 and p53. U2OS cells were exposed to CDDP (20 μM). Twenty-four hours after CDDP treatment, cell lysates prepared from U2OS cells were immunoprecipitated with NRS or with anti-NEDL1 antibody and analysed by immunoblotting with anti-p53 antibody (top panel). The anti-NEDL1 immunoprecipitates contained endogenous NEDL1 (middle panel). To show that equal amounts of cell lysates are used for immunoprecipitation, expression of actin was examined (bottom panel). (**c**) Mutant form of p53 does not bind to NEDL1. Human breast cancer MDA-MB-231 cells, in which Arg at 280 is substituted with Lys, were transfected with expression plasmid for NEDL1. Forty-eight hours after transfection, cell lysates were immunoprecipitated with polyclonal anti-NEDL1 antibody or with NRS and the immunoprecipitates were analysed by immunoblotting with the indicated antibodies. Ten percentage of inputs are also shown (input). (**d**) The indicated p53 derivatives were labeled with [^{35}S]methionine *in vitro* and incubated with cell lysates prepared from COS7 cells transfected with expression plasmid for NEDL1. The reaction mixtures were immunoprecipitated with anti-NEDL1 antibody and the immunoprecipitates were analysed by sodium dodecyl sulfate polyacrylamide gel electrophoresis. The gels were then dried and subjected to autoradiography. CDDP, cisplatin; NEDL1, NEDD4-like ubiquitin protein ligase-1; NRS, normal rabbit serum.

exposed to the indicated concentrations of ADR for 24 h followed by fluorescence-activated cell sorter (FACS) analysis. As shown in Figure 7b, U2OS cells transfected with control siRNA underwent apoptosis in a dose-dependent manner. In contrast, the number of cells with sub-G1 DNA content in response to ADR was significantly decreased in U2OS cells transfected with siRNAs against NEDL1 relative to cells expressing control siRNA. Similarly, siRNA-mediated knockdown of endogenous NEDL1 led to a remarkable decrease in the number of apoptotic cells caused by ADR in a time-dependent manner (Figure 7c).

Next, we determined whether siRNA-mediated knockdown of endogenous NEDL1 could inhibit the transcriptional activation of p53 target genes in response to ADR. U2OS cells were transfected with the indicated siRNAs. Twenty-four hours after transfection, cells were treated with ADR for 24 h. As shown in Figure 8a, ADR treatment induced the accumulation of p53 and phosphorylated form of p53 at Ser-15. However, siRNA-mediated knockdown of endogenous NEDL1 had negligible effects on amounts of p53 and phosphorylated form of p53 at Ser-15 in response to ADR, suggesting that their interaction does not affect the stability of p53 in response to DNA damage. It is noteworthy that expression levels of Noxa increased in cells exposed to ADR, whereas ADR-mediated upregulation of Noxa was markedly inhibited in NEDL1-knocked down U2OS cells. RT–PCR analysis also demonstrated that siRNA-mediated knockdown of endogenous NEDL1 reduces the transcription of p53 target genes such as *Noxa* and *Puma* induced by ADR (Figure 8b). ADR treatment had undetectable effects on *p53* (data not shown). Intriguingly, NEDL1 increased the acetylation levels of p73 (Figure 8c). Taken together, our present results suggest that NEDL1 has an ability to enhance the transcriptional and pro-apoptotic activities of p53 through the interaction without affecting its stability.

Discussion

In the present study, we have found that a novel HECT-type E3 ubiquitin ligase NEDL1 has the ability to cooperate with p53 to induce apoptosis.

During CDDP-mediated apoptosis in SH-SY5Y cells carrying wild-type *p53*, expression levels of NEDL1 correlated with those of p53. Expression levels of *NEDL1* were higher in favorable neuroblastoma than those in unfavorable neuroblastoma. Favorable neuroblastoma undergoes spontaneous regression through

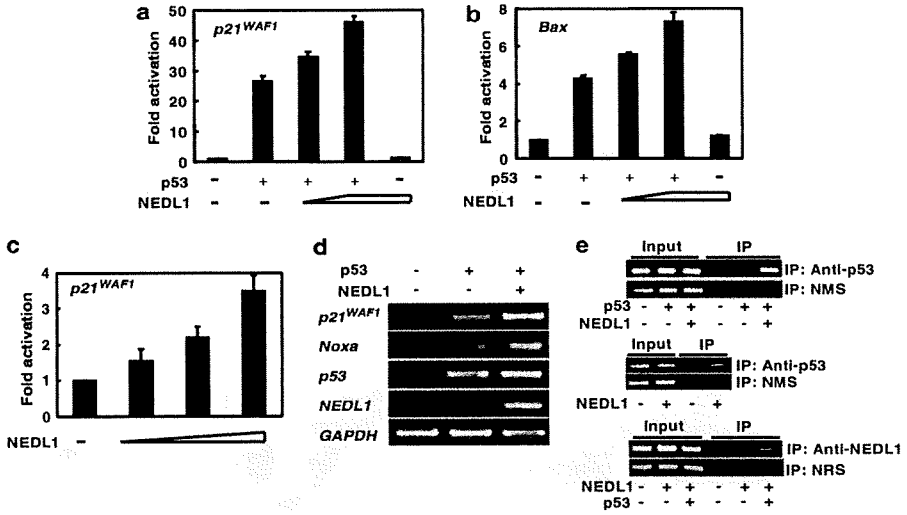

Figure 5 NEDL1 enhances the transcriptional activity of p53. (a and b) Luciferase reporter assays. H1299 cells were co-transfected with 25 ng of expression plasmid for p53, 100 ng of luciferase reporter construct containing p53-responsive element derived from *p21*^{WAF1} (a) or *Bax* (b) promoter and 10 ng of *Renilla* luciferase plasmid (pRL-TK) together with or without increasing amounts of expression plasmid for NEDL1 (475 and 875 ng). Total amount of plasmid DNA per transfection was kept constant (1 μg) with pcDNA3. Forty-eight hours after transfection, cell lysates were prepared and their luciferase activity was measured. Data were normalized to the *Renilla* luciferase activity. (c) Luciferase reporter assays. U2OS cells were co-transfected with 100 ng of luciferase reporter construct containing p53-responsive element derived from *p21*^{WAF1} promoter and 10 ng of pRL-TK together with or without increasing amounts of expression plasmid for NEDL1 (400, 800 and 1000 ng). Forty-eight hours after transfection, cell lysates were prepared and their luciferase activity was measured as described above. (d) RT PCR analysis. H1299 cells were co-transfected with a constant amount of p53 expression plasmid (0.1 μg) along with or without NEDL1 expression plasmid (1.9 μg). Forty-eight hours after transfection, total RNA was isolated and subjected to RT PCR analysis. *GAPDH* was used as an internal control. (e) ChIP assay. The increased binding of p53 to the promoter region of *p21*^{WAF1} caused by NEDL1 was demonstrated by ChIP assay with chromatin isolated from H1299 cells transfected with the indicated combinations of expression plasmids. As a control, PCR was performed on chromatin fragments isolated both before (input) and after (IP) immunoprecipitation with monoclonal anti-p53 antibody or with normal mouse serum (NMS) (upper panels). Middle panels show the increased binding of endogenous p53 to *p21*^{WAF1} promoter in the presence of NEDL1. Crosslinked chromatin isolated from U2OS cells transfected with or without NEDL1 expression plasmid exposed to adriamycin was subjected to ChIP assay. Lower panels show ChIP assay using crosslinked chromatin prepared from H1299 cells transfected with the indicated combinations of expression plasmids. Crosslinked chromatin was immunoprecipitated with polyclonal anti-NEDL1 or with NRS and subjected to PCR. CDDP, cisplatin; ChIP, chromatin immunoprecipitation; GAPDH, glyceraldehyde-3-phosphate dehydrogenase; NEDL1, NEDD4-like ubiquitin protein ligase-1; NRS, normal rabbit serum; RT PCR, reverse transcriptase PCR.

apoptosis and/or neuronal differentiation (Kitanaka *et al.*, 2002). In contrast to other human tumors, *p53* is rarely mutated in neuroblastoma (Moll *et al.*, 1995). Thus, it is likely that functional interaction between NEDL1 and p53 might contribute to induction of spontaneous regression caused by apoptosis of favorable neuroblastoma bearing wild-type *p53*. In support of this notion, enforced expression of NEDL1 reduced the number of drug-resistant colonies in cells with wild-type *p53* but not in *p53*-deficient cells. Furthermore, siRNA-mediated knockdown of endogenous NEDL1 inhibited DNA damage-induced apoptosis in cells bearing wild-type *p53*. Our present results demonstrated that NEDL1 binds to COOH-terminal region of p53 and enhances its transcriptional activation. In addition, NEDL1 increased the amounts of p53 recruited onto *p21*^{WAF1} promoter region. As described previously (Hupp and Lane, 1994), COOH-terminal region of p53 masked its DNA-binding domain to inhibit its transcriptional potential. Chemical modifications at COOH-terminal portion of p53, such as acetylation and glycosylation, lead to an increase in the transcriptional activity of p53 (Shaw *et al.*, 1996; Thomas and Chiang, 2005; Di Lello *et al.*, 2006). In accordance with this notion, enforced expression of NEDL1 resulted in an increase in acetylation levels of p53. Thus, it is possible that the interaction between NEDL1 and p53 might help to expose DNA-binding domain of p53 through the induction of acetylation of p53, and thereby enhance its transcriptional activity. However, the precise molecular mechanisms behind NEDL1-mediated induction of acetylation of p53 remained unclear. Further studies should be necessary to address this issue.

Although we found that NEDL1 has an intrinsic E3 ubiquitin ligase activity (Miyazaki *et al.*, 2004), our extensive efforts failed to detect NEDL1-mediated ubiquitination of p53 and enforced expression of NEDL1 had undetectable effects on the stability of endogenous p53 (data not shown). Under our experimental conditions, MDM2 promoted ubiquitination-mediated degradation of p53 (data not shown). NEDL1 and mutant form of NEDL1 lacking its catalytic HECT domain had an ability to decrease the number of drug-resistant colonies in H1299 cells co-transfected with p53 expression plasmid. Like wild-type NEDL1, this NEDL1 mutant retained an ability to interact with

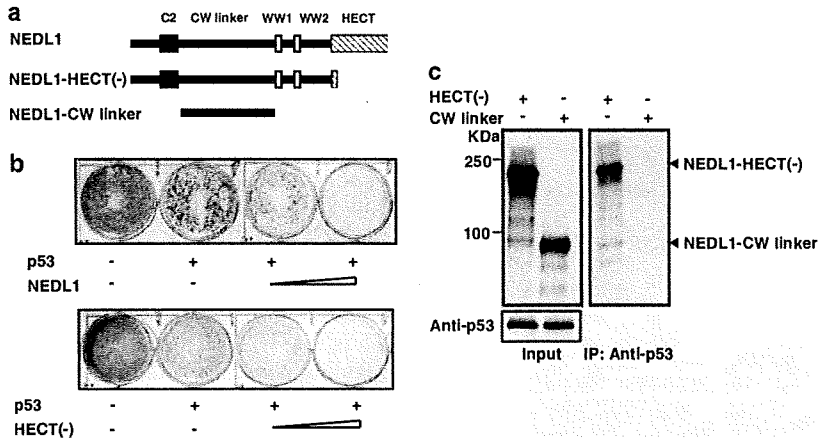

Figure 6 NEDL1 increases pro-apoptotic activity of p53 in its catalytic activity-independent manner. (a) Schematic diagram of wild-type NEDL1 and its deletion mutants. (b) Colony formation assay. H1299 cells were co-transfected with constant amount of p53 expression plasmid (25 ng) together with or without increasing amounts of expression plasmid for NEDL1 (475 and 975 ng) (upper panel) or NEDL1 lacking HECT domain (475 and 975 ng) (lower panel). Forty-eight hours after transfection, cells were grown in the fresh medium containing G418 (400 μg ml^{-1}). Following 2 weeks selection, drug-resistant colonies were stained with Giemsa's solution. (c) *In vitro* pull-down assay. Cell lysates prepared from COS7 cells were incubated with the indicated radio-labeled NEDL1 mutants and then immunoprecipitated with anti-p53 antibody. The immunoprecipitates were subjected to autoradiography (right panel). Left panel shows the autoradiography of the radio-labeled NEDL1 deletion mutants generated by *in vitro* transcription/translation system. NEDL1, NEDD4-like ubiquitin protein ligase-1.

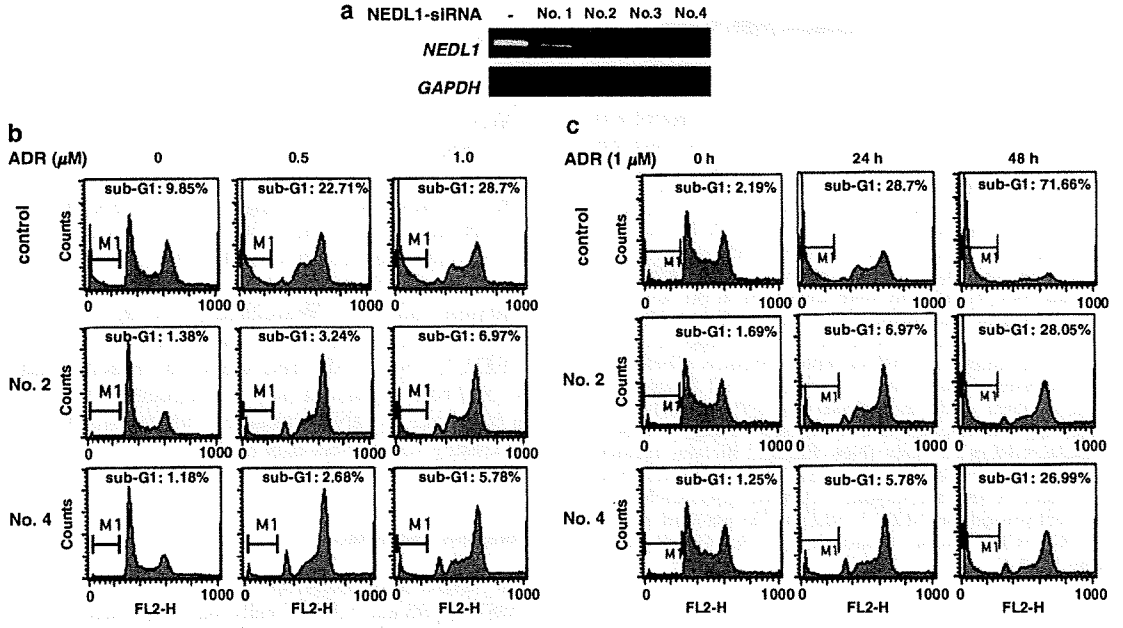

Figure 7 siRNA-mediated knockdown of endogenous NEDL1 confers resistance of U2OS cells to ADR. (a) siRNA-mediated knockdown of endogenous NEDL1. U2OS cells were transfected with control siRNA (−), siRNA against NEDL1 termed no. 1, 2, 3 or 4 siRNA. Forty-eight hours after transfection, total RNA was prepared and subjected to reverse transcriptase PCR. *GAPDH* was used as an internal control. (b) U2OS cells were transfected with control siRNA, no. 2 or 4 siRNA. Twenty-four hours after transfection, cells were exposed to the indicated concentrations of ADR for 24 h and then cell cycle distributions of cells were analysed by FACS. (c) U2OS cells were transfected with control siRNA, no. 2 or 4 siRNA. Twenty-four hours after transfection, cells were treated with ADR (1 μM). At the indicated time periods, cell cycle distributions of cells were analysed by FACS. ADR, adriamycin; GAPDH, glyceraldehyde-3-phosphate dehydrogenase; NEDL1, NEDD4-like ubiquitin protein ligase-1; siRNA, small interfering RNA.

p53 but not ubiquitinate p53. Thus, it is conceivable that the interaction of NEDL1 with p53 suppresses the inhibitory effect of COOH-terminal region of p53 on its function in its catalytic activity-independent manner.

In contrast to p53, NEDL1 did not interact with other p53 family members such as p73 and p63 (data not shown). Intriguingly, we reported that NEDL2, a close relative to NEDL1, binds to PY motif of p73 and

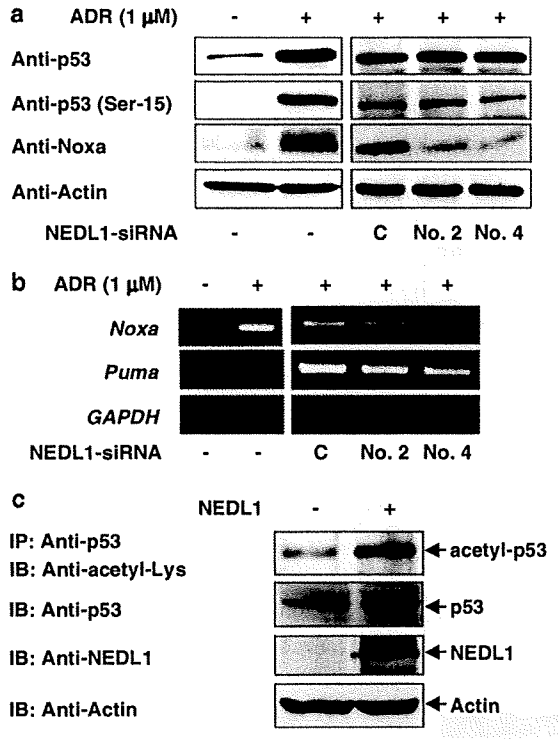

Figure 8 siRNA-mediated depletion of endogenous NEDL1 does not affect the stability of p53 but inhibits ADR-mediated upregulation of p53 target genes. (**a**) U2OS cells were treated with or without ADR (1 μM). Twenty-four hours after the treatment, cell lysates were prepared and subjected to immunoblotting with the indicated antibodies (left panels). U2OS cells were transfected with control siRNA (C), no. 2 or 4 siRNA. Twenty-four hours after transfection, cells were treated with ADR. At the indicated time periods, cell lysates were prepared and processed for immunoblotting with the indicated antibodies (right panels). (**b**) RT PCR analysis. U2OS cells were treated as in (**a**), and total RNA was prepared and subjected to RT PCR. (**c**) NEDL1-mediated increase in acetylation levels of p53. U2OS cells were transfected with empty plasmid or with expression plasmid for NEDL1. Forty-eight hours after transfection, cell lysates were immunoprecipitated with monoclonal anti-p53 antibody. The immunoprecipitates were analysed by immunoblotting with polyclonal anti-acetyl-Lys antibody (New England Biolabs, Ipswich, MA, USA). Expression levels of total p53, NEDL1 and actin were also examined. ADR, adriamycin; GAPDH, glyceraldehyde-3-phosphate dehydrogenase; NEDL1, NEDD4-like ubiquitin protein ligase-1; RT PCR, reverse transcriptase PCR; siRNA, small interfering RNA.

promotes ubiquitination of p73 (Miyazaki *et al.*, 2003). According to our previous results, NEDL2-mediated ubiquitination of p73 increased the stability and activity of p73, raising a possibility that ubiquitination does not always act as a degradation signal. Consistent with our results, ubiquitination was required for the transcriptional activity of c-myc (Adhikary *et al.*, 2005). It is noteworthy that NEDL2 did not interact with p53 that lacks PY motif and had negligible effects on p53 (Miyazaki *et al.*, 2003), indicating that NEDL1 family members have a differential effect on p53 family members. In this regard, it is of interest to examine whether there could exist a functional interaction between NEDL1 family members and p63 that contains PY motif.

Several lines of evidence suggest that pro-apoptotic p53 signaling pathway is involved in motor neuron death associated with amyotrophic lateral sclerosis through an upregulation of pro-apoptotic Bax (Ekegren *et al.*, 1999; Gonzalez de Aguilar *et al.*, 2000; Martin and Liu, 2002). Recently, it has been shown that Noxa is one of the critical mediators of p53-dependent motor neuron death (Kiryo-Seo *et al.*, 2005). These observations suggest that pro-apoptotic p53 signaling pathway plays a causable role in the regulation of neuronal cell death. Thus, it is likely that NEDL1 is involved in the regulation of this cellular process through the interaction with p53.

As described previously (Miyazaki *et al.*, 2004), we found that Dvl-1, a highly conserved cytoplasmic phosphoprotein implicated in Wnt signaling pathway, is one of the physiological targets of NEDL1. On the basis of our previous results, NEDL1 ubiquitinated Dvl-1 and induced its degradation in a proteasome-dependent manner. It has been well documented that Dvl-1 increases the stability of β-catenin through the inhibition of the catalytic activity of glycogen synthase kinase-3β (GSK-3β) (Kishida *et al.*, 2001; Lee *et al.*, 2001; Hino *et al.*, 2003). In addition, GSK-3β facilitated staurosporine-mediated apoptosis in SH-SY5Y cells (Bijur *et al.*, 2000) and also contributed to neuronal apoptosis induced by trophic withdrawal (Hetman *et al.*, 2000). Consistent with these results, specific inhibition of GSK-3β activity by a small chemical compound protected primary neuron from apoptosis (Cross *et al.*, 2001). These results suggest that GSK-3β activity is closely involved in the induction of neuronal cell death. It is worth noting that GSK-3β interacts with p53 in response to DNA damage and enhances pro-apoptotic function of p53 (Watcharasit *et al.*, 2002). Taken together, there exists a functional interaction among NEDL1, Dvl-1, p53 and GSK-3β, which might play a pivotal role at least in part in the regulation of apoptosis in response to DNA damage. Further studies should be necessary to address this issue.

Materials and methods

Cell culture and transfection

COS7, U2OS and SAOS-2 cells were maintained in Dulbecco's modified Eagle's medium supplemented with 10% of heat-inactivated fetal bovine serum (Invitrogen, Carlsbad, CA, USA), penicillin (100 IU ml^{-1}) and streptomycin (100 μg ml^{-1}). *p53*-deficient H1299 and SH-SY5Y cells were grown in RPMI-1640 medium supplemented with 10% heat-inactivated fetal bovine serum and antibiotic mixture. Cells were cultured at 37 °C in a water-saturated atmosphere of 95% air and 5% CO_2. Transient transfection was performed using LipofectAMINE 2000 transfection reagent (Invitrogen) according to the manufacturer's instructions.

Immunoblotting and immunoprecipitation

For immunoblotting, cells were lysed in a lysis buffer containing 25 mM Tris-Cl pH 7.5, 137 mM NaCl, 2.7 mM

KCl, 1% Triton X-100 and protease inhibitor cocktail. Equal amounts of cell lysates were separated by sodium dodecyl sulfate–polyacrylamide gel electrophoresis (SDS–PAGE) and transferred onto Immobilon-P membranes (Millipore, Bedford, MA, USA). The transferred membranes were incubated with monoclonal anti-p21^{WAF1} (Ab-1, Oncogene Research Products, Cambridge, MA, USA), monoclonal anti-p53 (DO-1, Oncogene Research Products), monoclonal anti-Noxa (ab13654, Abcom, Cambridge, UK), polyclonal anti-Bax (Cell Signaling, Beverly, MA, USA), polyclonal anti-caspase-3 (Calbiochem, San Diego, CA, USA), polyclonal anti-phosphorylated p53 at Ser-15 (Cell Signaling), polyclonal anti-NEDL1 or with polyclonal anti-actin (20–33, Sigma, St Louis, MO, USA) antibody followed by incubation with the appropriate HRP-conjugated secondary antibodies (Jackson ImmunoResearch Laboratories, West Grove, PA, USA). Bound antibodies were detected by ECL system (Amersham Biosciences, Piscataway, NJ, USA). For immunoprecipitation, 1 mg of protein was incubated with protein G-Sepharose beads (Amersham Biosciences). The precleaned lysates were incubated with polyclonal anti-NEDL1 antibody for 2 h at 4 °C and immunocomplexes were precipitated with protein G-Sepharose beads for additional 1 h at 4 °C. The immunocomplexes were washed three times with the lysis buffer, eluted from beads by adding 2 × SDS sample buffer, resolved by SDS–PAGE and subjected to immunoblotting with polyclonal anti-NEDL1 or with monoclonal anti-p53 (DO-1, Oncogene Research Products) antibody.

In vitro *binding assay*
Wild-type p53 and its deletion mutants were expressed *in vitro* using a T7 Quick Coupled Transcription/Translation System (Promega, Madison, WI, USA) in the presence of [^{35}S]methionine according to the manufacturer's recommendations. Cell lysates prepared from COS7 cells transfected with the expression plasmid encoding NEDL1 were mixed and incubated overnight at 4 °C. Reaction mixtures were then immunoprecipitated with the anti-NEDL1 antibody. Immunoprecipitates were washed extensively with the lysis buffer and resolved by SDS–PAGE. The gels were dried and subjected to autoradiography.

TUNEL assay
SH-SY5Y cells were grown on coverslips and treated with CDDP (20 μM). At the indicated time periods after the treatment with CDDP, cells were fixed in 4% paraformaldehyde and apoptotic cells were detected by using an *in situ* cell death detection Kit (Roche Molecular Biochemicals, Mannheim, Germany) according to the manufacturer's protocol. The coverslips were mounted with 4′,6-diamidino-2-phenylindole-containing mounting medium (Vector Laboratories, Burlingame, CA, USA) and observed under a Fluoview laser scanning confocal microscope (Olympus, Tokyo, Japan).

FACS analysis
U2OS and SAOS-2 cells were transfected with the expression plasmid for NEDL1. Forty-eight hours after transfection, floating and attached cells were collected, washed in phosphate-buffered saline and fixed in 70% ethanol at −20 °C. Following incubation in phosphate-buffered saline containing 40 μg ml^{-1} of propidium iodide and 200 μg ml^{-1} of RNase A for 1 h at room temperature in the dark, stained nuclei were analysed on a FACScan machine (Becton Dickingson, Mountain View, CA, USA).

RT–PCR
SH-SY5Y cells were treated with CDDP (20 μM). At the indicated time periods after the treatment, total RNA was prepared using an RNeasy mini kit (Qiagen, Valencia, CA, USA). Five micrograms of total RNA were employed to synthesize the first-strand cDNA by using random primers and SuperScript II reverse transcriptase (Invitrogen) according to the manufacturer's instructions. The resultant cDNA was subjected to the PCR-based amplification. The list of primer sets used will be provided upon request. The expression of glyceraldehyde-3-phosphate dehydrogenase was measured as an internal control. The PCR products were subjected to agarose gel electrophoresis and visualized by ethidium bromide staining.

Luciferase reporter assay
H1299 cells were allowed to adhere overnight in 12-well cell culture plates at a final density of 50 000 cells per well. Cells were then co-transfected with 25 ng of the p53 expression plasmid, 100 ng of the p53-responsible luciferase reporter construct (*p21^{WAF1}* or *Bax*) and 10 ng of pRL-TK *Renilla* luciferase cDNA together with or without increasing amounts of the NEDL1 expression plasmid (475 and 875 ng). Total amount of plasmid DNA per transfection was kept constant (1 μg) with an empty plasmid pcDNA3 (Invitrogen). Forty-eight hours after transfection, cells were lysed and both the firefly and *Renilla* luciferase activities were measured with dual-luciferase reporter assay system (Promega), according to the manufacturer's instructions. The firefly luminescence signal was normalized based on the *Renilla* luminescence signal.

Chromatin immunoprecipitation assay
Chromatin immunoprecipitation assay was performed according to the protocol provided by Upstate Biotechnology (Lake Placid, NY, USA). In brief, H1299 cells were transfected with the expression plasmid for p53 together with or without the expression plasmid for NEDL1. Forty-eight hours after transfection, cells were treated with 1% formaldehyde at 37 °C for 15 min. After being washed with ice-cold phosphate-buffered saline, cells were suspended with 200 μl of SDS lysis buffer (1% SDS, 10 mM EDTA and 50 mM Tris-HCl, pH 8.1) on ice for 10 min. Lysates were sonicated and insoluble materials were removed by centrifugation. Supernatants were then precleared with 20 μl of protein A agarose beads that had been preabsorbed with salmon sperm DNA at 37 °C for 30 min. The precleared chromatin solutions were immunoprecipitated with normal mouse serum or with anti-p53 antibody at 4 °C overnight, followed by incubation with 60 μl of protein A agarose beads for 1 h at 4 °C. Samples were eluted with 200 μl of the elution buffer (1% SDS and 0.1 M $NaHCO_3$) and then crosslinks were reversed by heating them at 65 °C for 6 h. Chromatin-associated proteins were digested with proteinase K at 45 °C for 1 h, and immunoprecipitated DNA was purified by using QIAquick PCR purification kit (Qiagen) according to the manufacturer's instructions. Purified DNA was analysed by PCR-based amplification. The primer set used to detect *p21^{WAF1}* promoter was as follows: 5′-CACCTTTCACCAT TCCCCTA-3′ (forward) and 5′-GCAGCCCAAGGACAAA ATAG-3′ (reverse).

Small interfering RNA
U2OS cells were transiently transfected with siRNA targeting NEDL1 (no. 1, 5′-CUAAAUGACUGGCGGAAUAUU-3′; no. 2, 5′-GAUGAGGUCUUGUCCGAAAUU-3′; no. 3, 5′-GAUGCCAGCUCGUACUUUGUU-3′; no. 4, 5′-CAGCU GCAAUUCCGAUUUGUU-3′) or control non-targeting